

Design, synthesis and biological evaluation of 3-hydroxyquinazoline-2,4(1*H*,3*H*)-diones as dual inhibitors of HIV-1 reverse transcriptase-associated RNase H and integrase

Ping Gao^a, Xiqiang Cheng^a, Lin Sun^a, Shu Song^a, Mar Álvarez^b, Joanna Luczkowiak^b, Christophe Pannecouque^c, Erik De Clercq^c, Luis Menéndez-Arias^{b,*}, Peng Zhan^{a,*}, Xinyong Liu^{a,*}

^aDepartment of Medicinal Chemistry, Key Laboratory of Chemical Biology, Ministry of Education, School of Pharmaceutical Sciences, Shandong University, Ji'nan, 250012

^bCentro de Biología Molecular “Severo Ochoa” (Consejo Superior de Investigaciones Científicas & Universidad Autónoma de Madrid), Madrid, Spain

^cRega Institute for Medical Research, KU Leuven, Minderbroedersstraat 10, B-3000 Leuven, Belgium

*E-mail: lmenendez@cbm.csic.es (Menéndez-Arias L.); zhanpeng1982@sdu.edu.cn (Zhan P.); xinyongl@sdu.edu.cn (Liu X.Y.).

Abstract

A novel series of 3-hydroxyquinazoline-2,4(1*H*,3*H*)-diones derivatives has been designed and synthesized. Their biochemical characterization revealed that most of the compounds were effective inhibitors of HIV-1 RNase H activity at sub to low micromolar concentrations. Among them, II-4 was the most potent in enzymatic assays, showing an IC₅₀ value of 0.41 ± 0.13 μM, almost five times lower than the IC₅₀ obtained with β-thujaplicinol. In addition, II-4 was also effective in inhibiting HIV-1 IN strand transfer activity (IC₅₀ = 0.85 ± 0.18 μM) but less potent than raltegravir (IC₅₀ = 71 ± 14 nM). Despite its relatively low cytotoxicity, the efficiency of II-4 in cell culture was limited by its poor membrane permeability. Nevertheless, structure-activity relationships and molecular modeling studies confirmed the importance of tested 3-hydroxyquinazoline-2,4(1*H*,3*H*)-diones as useful leads for further optimization.

Key words: HIV-1, RNase H, integrase, dual inhibitors

1. Introduction

HIV/AIDS continues to be a major global health epidemic. In 2017, there were 36.9 million people living with HIV worldwide and an additional 1.8 million people became newly infected [1]. Although combinations of anti-HIV drugs targeting different steps of the viral replication cycle are effective in maintaining a very low or undetectable viral load in infected patients, shortcomings of antiretroviral therapies include their adverse side effects, the emergence of extensively cross-resistant strains of HIV-1, high cost of most effective therapies, and limited availability in many countries around the world. In this scenario, novel therapeutics that act on previously untargeted

steps of the viral life cycle are urgently needed to circumvent the onset of drug resistance and to improve current treatments [2].

The HIV-1 reverse transcriptase (RT) is a validated target for AIDS therapy. RT plays an essential role in virus replication. It converts the viral single-stranded genomic RNA into double-stranded proviral DNA that integrates into the host cell's genome. During this process, the DNA polymerase activity of the RT synthesizes the proviral DNA, while the RT's RNase H activity degrades the viral RNA genome used as template during DNA synthesis [3, 4]. Interestingly, RT DNA polymerase nucleoside RT inhibitors (NRTIs) constitute the backbone of current therapies, and several non-nucleoside RT inhibitors (NNRTIs) are widely used in the clinical setting. However, drug discovery efforts to obtain RT RNase H inhibitors have not provided any promising candidate currently in development. Therefore, RNase H represents a novel and attractive target for antiretroviral drug development, potentially useful to treat HIV variants resistant to current drugs.

The RNase H active site contains a highly conserved DEDD motif consisting of four carboxylated amino acid residues in close proximity (Asp443, Glu478, Asp498 and Asp549) that interact with two metal ions (Mg^{2+}) [5]. A similar arrangement is observed in the active site of HIV-1 IN, another metalloenzyme that plays critical roles in viral infection and the establishment of proviral latency. Three highly conserved residues in the catalytic core domain of the enzyme, namely, Asp64, Asp116, and Glu152 (DDE motif) coordinate the two divalent cations necessary for its strand transfer activity [6]. The geometries of the catalytic sites of HIV-1 RNase H and IN are similar with their active site residues and magnesium ions located at structurally equivalent positions in both enzymes. In addition, dual inhibitors of both enzymes have been previously described [7, 8].

Continued efforts in medicinal chemistry and clinical testing have led to the approval of four HIV-1 IN inhibitors: raltegravir (RAL), elvitegravir (EVG), dolutegravir (DTG), and bictegravir [3, 9-13], while several chemotypes targeting the RNase H active site, and inhibiting its endonuclease activity at sub to low micromolar concentration have been described [14-17] (Fig.1).

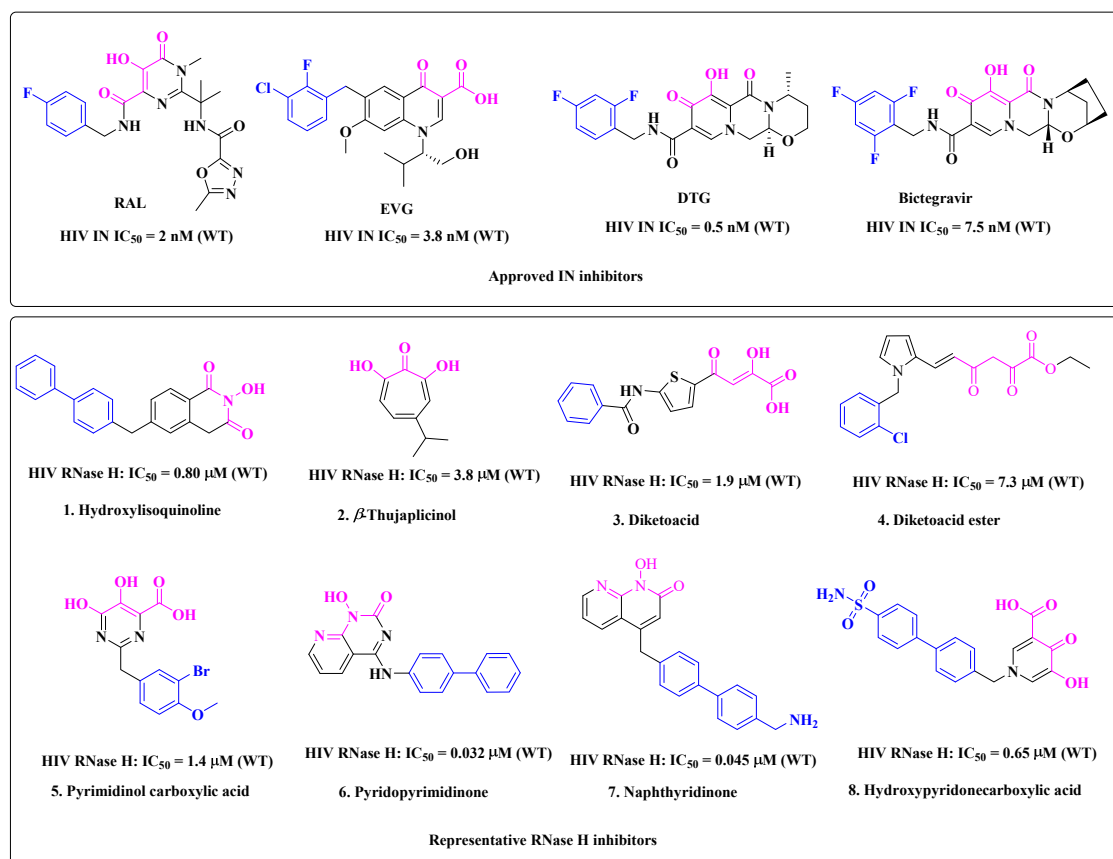
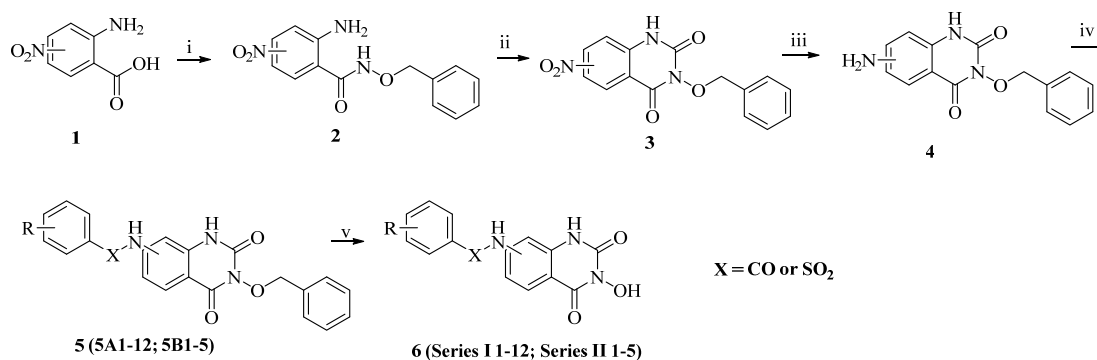


Fig.1 Approved IN inhibitors and representative RNase H inhibitors. IC₅₀ values for HIV-1 IN strand transfer and RNase H inhibition assays using purified enzymes are shown below.

Hybridization of hydroxyisoquinoline (HID) and hydroxypyrimidine-2,4-dione (HPD) scaffolds led to the design of 3-hydroxyquinazoline-2,4(1*H*,3*H*)-diones. This chemotype is similar to that of *N*-hydroxyureas, initially described as inhibitors of flap endonuclease-1 [18]. The HIV-1 RNase H inhibitory activity of 3-hydroxyquinazoline-2,4(1*H*,3*H*)-diones has been recently reported by Kankanala *et al.*, although their assessment was limited to compounds 6-(4-chlorophenyl)-3-hydroxyquinazoline-2,4(1*H*,3*H*)-dione and 3-hydroxy-6-phenylquinazoline-2,4(1*H*,3*H*)-dione [19]. In the current study, we obtained a new series of 3-hydroxyquinazoline-2,4(1*H*,3*H*)-diones, designed by introducing different benzamide or phenylsulfonamide substituents at positions 6 and 7 of the quinazoline ring. The new compounds were synthesized through simple and convenient procedures in order to explore their structure-activity relationships (SAR), and improve their inhibitory properties.

2. Results and Discussion

2.1. Chemistry



Scheme 1. Reaction reagents and conditions: i) *O*-benzylhydroxylamine, *N,N*-carbonyldiimidazole, tetrahydrofuran, 60 °C, 5 h; ii) triphosgene, triethylamine, tetrahydrofuran, room temperature, 1 h; iii) iron powder, chlorination ammonium, ethanol, reflux, 2 h; iv) corresponding benzoyl chloride or benzenesulfonyl chloride, pyridine, 0 °C, 3 h; v) H₂, Pd/C, room temperature, 1 h.

The target compounds were prepared by following a relatively simple procedure outlined in Scheme 1. By treating commercially available methyl 4-nitroanthranilic acid or 5-nitroanthranilic acid (**1**) with *O*-benzylhydroxylamine and *N,N*-carbonyldiimidazole in tetrahydrofuran (THF), compound **2** was obtained. Then, a cyclization step using triphosgene yielded the intermediate **3**. After nitro reduction to obtain compound **5**, followed by acylation to get compound **6**, the desired compounds were obtained by hydrogenolytic deprotection of their *N*-hydroxyl group.

2.2 Biological activity

2.2.1. Inhibition of HIV-1 RNase H activity

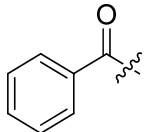
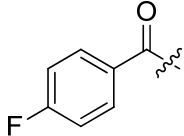
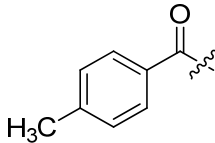
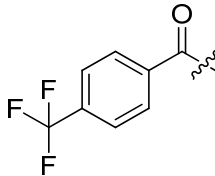
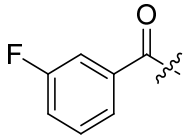
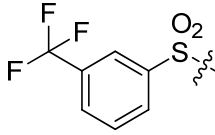
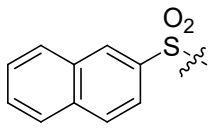
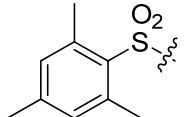
All newly synthesized compounds were tested *in vitro* for their inhibitory activity against the RNase H of HIV-1 RT, and products of the endonucleolytic reaction were analyzed by denaturing polyacrylamide gel electrophoresis [20]. Overall, series **I-II** were all potent RNase H inhibitors with IC₅₀ values ranging from 0.41 to 20.1 μM (Table 1). Compound **II-4** was the most active derivative of this series, with IC₅₀ value of 0.41 ± 0.13 μM. It was almost 5 times more potent than the reference compound β-thujaplicinol (IC₅₀ = 1.98 ± 0.22 μM) in these assays. **I-7** was found to be the worst inhibitor of the series with an IC₅₀ value of 20.1 ± 10.4 μM. The naphthyl group of compounds **II-4** and **I-7** was located at positions 6 and 7, respectively. These differences were

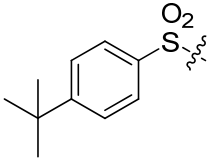
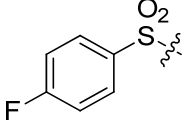
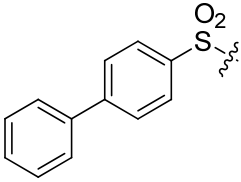
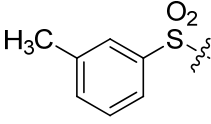
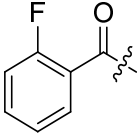
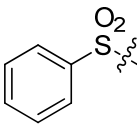
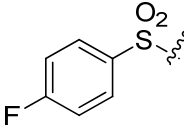
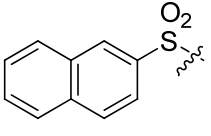
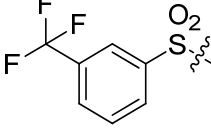
responsible for the 50-fold reduction in RNase H inhibition found for **I-7** as compared to **II-4**.

The comparison of RNase H inhibitory activities of compounds having substituents at position 7 (series 1: **I-1** to **I-12**) revealed that the activities of derivatives with benzoyl substitutions were slightly higher than those obtained with molecules having a benzenesulfonyl substitution. Among the compounds having benzoyl substituents (**I-1** to **I-5**), the least substituted compound (**I-1**) was also the best of this small series, with an IC_{50} value of $2.52 \pm 0.78 \mu\text{M}$. The effects of substitutions in the benzyl group in these compounds followed the order: none (**I-1**) > 4-methyl (**I-3**) > 4-F (**I-2**) \approx 3-F (**I-5**) > 4-CF₃ (**I-4**), although differences were not relevant in most cases. **I-4** was the least potent compound of the group. Regarding the benzenesulfonyl substitution derivatives (**I-6** to **I-12**), the naphthyl derivative (**I-7**, IC_{50} value of $20.1 \pm 10.4 \mu\text{M}$) was the least active compound. The order of potency of these compounds was: 2,4,6-triCH₃ phenyl (**I-8**) > 3-CH₃ phenyl (**I-12**) > 3-CF₃ phenyl (**I-6**) > 4-F phenyl (**I-10**) > 4-tert-butyl phenyl (**I-10**) > biphenyl (**I-11**) > naphthyl (**I-7**).

The activity of the 6-substituted compounds (compounds **II-1** to **II-5**) was significantly higher than that of the 7-substituted compounds. Series II compounds with benzenesulfonyl substitutions were more potent inhibitors than the one with the benzoyl substitution (**II-1**). The naphthyl derivative (**II-4**, IC_{50} value of $0.41 \pm 0.13 \mu\text{M}$) was the most active compound. The order of potency of the benzenesulfonyl derivatives of series II was: naphthyl (**II-4**) > phenyl (**II-2**) > 3-CF₃ phenyl (**II-5**) > 4-F phenyl (**II-3**).

Table 1. RNase H inhibitory activity, anti-HIV activity and cytotoxicity in MT-4 cells.

		Series I		Series II			
Compounds	R	IC ₅₀ (μM)		EC ₅₀ (μM) ^b		CC ₅₀ (μM) ^c	
		RNase H ^a		IIIB	ROD		
I-1		2.52 ± 0.78		>36.6	>36.6	36.6 ± 11.4	
I-2		3.73 ± 0.94		>43.0	>43.0	43.0 ± 4.9	
I-3		2.74 ± 0.98		>10.9	>10.9	10.9 ± 3.1	
I-4		6.09 ± 2.53		>315.9	>315.9	315.9 ± 18.6	
I-5		3.73 ± 1.04		>39.8	>39.8	39.8 ± 3.4	
I-6		5.33 ± 1.76		>80.2	>80.2	80.2 ± 28.4	
I-7		20.1 ± 10.4		>219.6	>219.6	219.6 ± 3.1	
I-8		3.24 ± 1.26		>153.5	>153.5	153.5 ± 47.4	

I-9		5.88 ± 3.04	>307.0	>307.0	307.0 ± 9.4
I-10		5.68 ± 2.71	>355.8	>355.8	>355.8
I-11		11.7 ± 5.5	>305.3	>305.3	>305.3
I-12		4.10 ± 1.61	>309.5	>309.5	309.5 ± 18.9
II-1		4.29 ± 0.96	>167.7	>167.7	167.7 ± 52.9
II-2		1.19 ± 0.31	>213.4	>213.4	213.4 ± 9.0
II-3		2.25 ± 0.85	>199.4	>199.4	199.4 ± 7.7
II-4		0.41 ± 0.13	>208.4	>208.4	208.4 ± 5.2
II-5		2.00 ± 0.81	>176.1	>176.1	176.1 ± 7.1
Raltegravir	-	^d	0.015±0.0024	0.020±0.0064	6.51 ± 0.15
β-thujaplicinol	-	1.98 ± 0.22	>2.83	>2.83	2.83 ± 0.46

^aConcentration required to inhibit by 50% the *in vitro* RNase H activity.

^bThe 50% effective antiviral concentration (EC₅₀) was defined as the concentration of the tested

compound achieving 50% protection from viral cytopathicity.

^cThe 50% cytotoxic concentration (CC₅₀) was defined as the compound concentration that reduced the viability of mock-infected cell cultures by 50%, as determined by the MTT method.

^dNot determined.

2.2.2 HIV-1 IN strand transfer inhibition

Based on the similarity of the HIV-1 RNase H and IN active sites, and the expected chelating activity of designed compounds, we determined the inhibitory activity of selected compounds (i.e. **I-7**, **I-9** and **II-4**) in IN strand transfer assays [21]. As shown in Fig. 2, the three compounds were able to inhibit the viral IN. Despite being ten times less potent than raltegravir (IC₅₀ = 71 ± 14 nM), **II-4** was found to be more potent than **I-7** and **I-9** in IN strand transfer assays, with an IC₅₀ value of 0.85 ± 0.18 μM. All three tested 3-hydroxyquinazoline-2,4(1*H*,3*H*)-diones were found to be effective inhibitors of both HIV-1 IN and RNase H activities. **I-7** and **I-9** were around ten times less potent than **II-4**, showing 50-60% inhibitory activity at 10 μM in HIV-1 IN strand transfer reactions. Interestingly, RNase H IC₅₀ values for **I-7** and **I-9** shown in Table 1 (20.1 ± 10.4 μM for **I-7** and 5.88 ± 3.04 μM for **I-9**) were in the same order of magnitude and 14-49 times higher than those obtained for **II-4**.

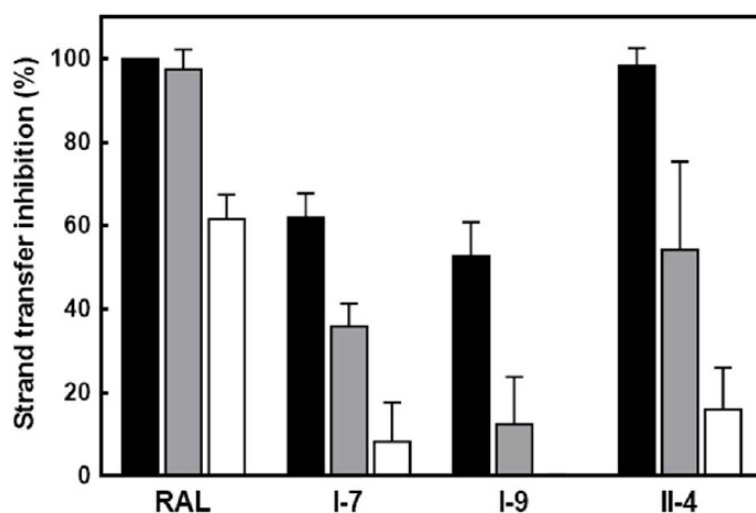


Fig. 2. HIV-1 IN strand transfer inhibition assays. Histograms represent percent inhibition of the strand transfer reaction in assays carried out with heteropolymeric hybrids in the presence of compounds I-7, I-9 and II-4 and raltegravir, at 10 μM, 1 μM and 0.1 μM concentrations (black, grey and white bars, respectively). RAL, raltegravir.

2.2.3 In vitro anti-HIV assay

All compounds were evaluated in cell culture for their antiviral activity against wild-type HIV-1 and HIV-2 strains (IIIB and ROD, respectively). Raltegravir was used as the reference drug for IN inhibition. EC₅₀ values (anti-HIV activity) and CC₅₀ values (cytotoxicity) are given in Table 1. At the highest concentration tested, series **I** and **II** compounds showed low toxicity, although none of them revealed significant HIV-1 replication inhibitory activity. The lack of inhibitory effect in cell culture curbed their potential development into antiviral drugs.

Table 2. Predicted physicochemical properties of compound **II-4**.^a

Physicochemical property	Tolerance limit	II-4
Number of atoms excluding hydrogens	-	27
Molecular weight	< 500 Da	383.38
Number of hydrogen bond acceptors	≤ 10	8
Number of hydrogen bond donors	≤ 5	3
Number of rotatable bonds	≤ 10	3
Total polar surface area	< 140 Å ²	121.26
Molecular volume	-	303.61
Octanol-water partition coefficient (log <i>P</i>)	< 5	2.30

^a Values determined using on-line cheminformatics software: <http://www.molinspiration.com/>

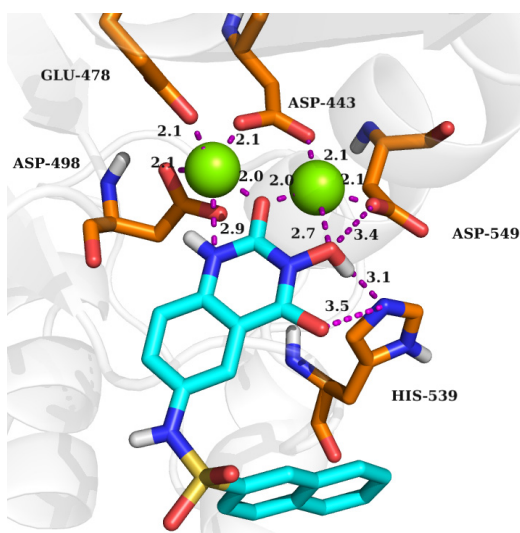
The reasons that explained the lack of activity of the tested compounds in cell culture was investigated. An overall assessment of the physicochemical properties of compound **II-4** using a free online software revealed that the compound could theoretically meet the general requirements accepted for useful drugs (Table 2), since size, polarity, volume and potentially reactive groups of **II-4** were below the tolerance limit. However, cell permeability assays were carried out and revealed that **II-4** had poor membrane permeability. Thus, in experiments carried out with Caco-2 cells, the apparent permeability (P_{app}) of **II-4** was below 1.9×10^{-7} cm/s, while reference compounds for low and high permeability, such as nadolol and metoprolol, showed P_{app} values of 9×10^{-8} cm/s and 1.47×10^{-5} cm/s, respectively. However, for **II-4**, the signal responses in receiver samples were lower than the limit of detection of the apparatus, and a precise calculation of P_{app} was not possible. The reported P_{app} ($< 1.9 \times 10^{-7}$ cm/s) was obtained by assuming the lowest detectable value in the receiver

chamber of our system (i.e. 50). In our assay conditions, recovery of **II-4** was sufficient and well above the 50% cut-off value, considered as sufficient for reliable estimates of P_{app} .

2.3. Molecular modeling analysis

To improve our understanding of structure-affinity relationships, the best compound of the series (i.e **II-4**) was docked in the structures of the HIV-1 RT RNase H domain (PDB code: 5J1E) and the prototype foamy virus (PFV) IN (PDB code: 3OYA), using the Surflex-Dock SYBYL-X 2.0 software. We used PFV IN as a surrogate model for HIV-1 IN, based on their high homology [22, 23]. The results of the docking analysis showing the theoretical binding location of **II-4** and its conformation are shown in Fig. 3.

According to these predictions, compound **II-4** binding within the RNase H active site suggests a potential interaction between the chelating triad of the 3-hydroxyquinazoline-2,4(1*H*,3*H*)-dione derivative and the two Mg^{2+} ions, which are coordinated to the conserved active site acidic residues Asp443, Glu478, Asp498, and Asp549 (Fig. 3A). The 3-hydroxyl group and the keto substituent at position 4 of **II-4** could establish hydrogen bonds with His539, which would stabilize the inhibitor near the active site metal-chelating residues forming the DEDD motif, all of them required for RNase H activity.



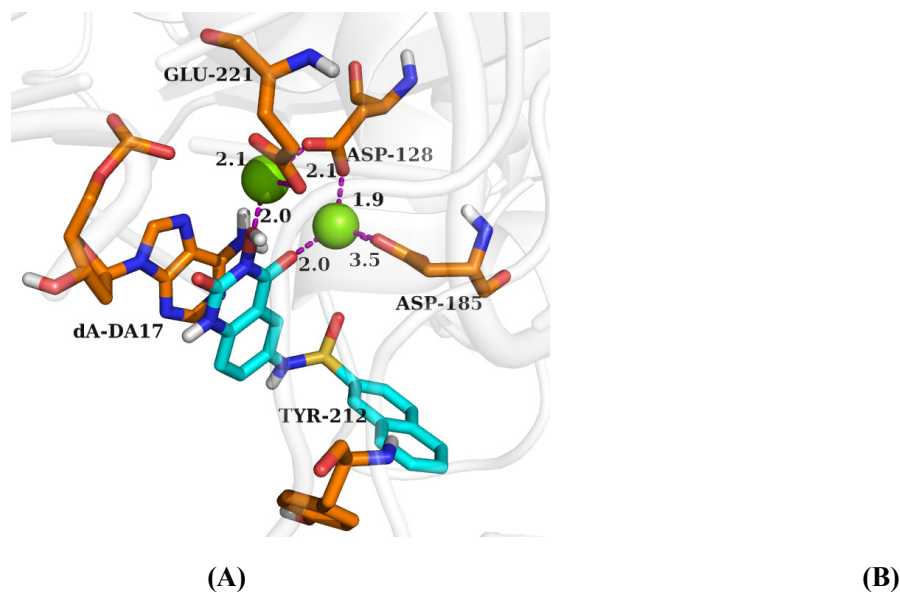


Fig. 3. Predicted binding modes of **II-4** (cyan) in the HIV-1 RNase H active site (A, PDB code: 5J1E) and the PFV IN active site (B, PDB code: 3OYA). Amino acid residues important for ligand binding are represented as sticks in orange. Magnesium ions are depicted as green spheres. Chelating and H-bond interactions are indicated by purple dashed lines. Hydrogens (nonpolar) are not shown. Figures were prepared with the PyMOL visualization program (<http://www.pymol.org>). Interatomic distances for key interactions are indicated in Å.

The predicted binding mode of compound **II-4** within the IN active site (Fig. 3B) shows chelating interactions between the chemotype core of the 3-hydroxyquinazoline-2,4(1*H*,3*H*)-dione and the two Mg²⁺ ions, coordinated by the highly conserved residues (Asp128, Asp185 and Glu221) in the active site of the enzyme. Besides, the rings containing the chelating triad of **II-4** form stacking interactions with the conserved terminal deoxyadenosine, located in the DNA. These interactions have been also observed in IN bound to approved strand transfer inhibitors such as raltegravir [22, 23]. In addition, the naphthyl moiety of **II-4** could participate in π -stacking interactions with the side-chain of Tyr212. All mentioned interactions seem to be important to justify the IN strand transfer inhibitory activity of **II-4**.

The binding models predicted for both RNase H and IN structures are consistent with our results showing that **II-4** is a potent HIV-1 RNase H-IN dual inhibitor, and provide support for further rational drug optimization.

3. Conclusion

Most of the 3-hydroxyquinazoline-2,4(1*H*,3*H*)-dione derivatives described in this study were

highly effective in inhibiting HIV-1 RNase H activity at sub to low micromolar concentrations. Among them, compound **II-4** was the most promising one with potent inhibitory activity against HIV-1 RNase H ($IC_{50} = 0.41 \pm 0.13 \mu\text{M}$), about five times more potent than β -thujaplicinol in enzymatic assays. Although less potent than the approved drug raltegravir, **II-4** turned out to be also a potent HIV-1 IN inhibitor with IC_{50} value of $0.85 \pm 0.18 \mu\text{M}$, providing further evidence of the feasibility of identifying dual HIV-1 RNase H-IN inhibitors through further modification of the 3-hydroxyquinazoline-2,4(1*H*,3*H*)-dione chemotype. Molecular modeling-based predictions revealed expected binding conformations for dual RNase H-IN inhibitors with the ambident chelating scaffold. Unfortunately, and despite their low cytotoxicity, herein described compounds failed to exhibit significant inhibitory activity in infected cells, probably in part due to their poor cell membrane permeability.

4. Experimental section

4.1. Synthetic procedures and analytical data

Mass spectrometry was performed on an API 4000 triple quadrupole mass spectrometer (Applied Biosystems/MDS Sciex, Concord, ON, Canada). ^1H NMR and ^{13}C NMR spectra were recorded on a Bruker AV-400 spectrometer (Bruker BioSpin, Switzerland), using solvents as indicated (DMSO- d_6). Chemical shifts were reported in δ values (ppm) with tetramethylsilane as the internal reference, and J values were reported in hertz (Hz). Melting points (mp) were determined on a micromelting point apparatus (Tian Jin Analytical Instrument Factory, Nankai, Tianjin, China). Flash column chromatography was performed on columns packed with silica gel 60 (200-300 mesh) (Qingdao waves silica gel desiccant co., Ltd, Qingdao, China). Thin layer chromatography was performed on pre-coated HUANGHAI® HSGF254, 0.15-0.2 mm TLC-plates (Yantai Jiangyou Silica Gel Development Co., Ltd., Yantai, Shandong, China). The key reactants including 4-nitroanthranilic acid, 5-nitroanthranilic acid, *O*-benzylhydroxylamine, *N,N*-carbonyldiimidazole etc. were purchased from Bide pharmatech Co. Ltd.

4.1.1. General procedure for the synthesis of 2-amino-*N*-(benzyloxy)-4-nitrobenzamide or 2-amino-*N*-(benzyloxy)-5-nitrobenzamide

A mixture of 2-amino-4-nitrobenzoic acid or 2-amino-5-nitrobenzoic acid (0.50 g, 2.7 mmol) with *N,N*-carbonyldiimidazole (0.55 g, 3.4 mmol, 1.25 eq), *O*-benzylhydroxylamine (470 μL , 4.1

mmol, 1.5 eq) in tetrahydrofuran was heated at 60 °C under agitation for 5 h. The reaction mixture was concentrated in vacuo and the residue was purified by silica gel chromatography using ethyl acetate and petroleum ether (eluent: petroleum ether: ethyl acetate = 12:1) to provide 2 as a yellow solid.

2-Amino-*N*-(benzyloxy)-4-nitrobenzamide: Yellow solid, 66% yield, mp: 163-165 °C.

2-Amino-*N*-(benzyloxy)-5-nitrobenzamide: Yellow solid, 78% yield, mp: 150-152 °C.

4.1.2. General procedure for the synthesis of 3-(benzyloxy)-6-nitroquinazoline-2,4(1H,3H)-dione or 3-(benzyloxy)-7-nitroquinazoline-2,4(1H,3H)-dione (3)

Triethylamine (603 µL, 4.35 mmol) was added dropwise to a solution of 2-amino-*N*-(benzyloxy)-4-nitrobenzamide or 2-amino-*N*-(benzyloxy)-5-nitrobenzamide (0.50 g, 1.74 mmol) and triphosgene (206 mg, 0.70 mmol) in anhydrous tetrahydrofuran (20 mL). The mixture was stirred at room temperature for 1–4 h, and then it was diluted with water (about 50 mL) to give a solid which was collected, washed with water, and recrystallized.

3-(Benzyloxy)-7-nitroquinazoline-2,4(1H,3H)-dione. Light yellow solid, 50% yield, mp: 271-272 °C. ¹H NMR (400 MHz, DMSO-*d*₆) δ 11.76 (s, 1H), 7.89 (d, *J* = 8.4 Hz, 1H), 7.59 – 7.55 (m, 2H), 7.46 – 7.40 (m, 4H), 7.38 (d, *J* = 1.8 Hz, 1H), 5.10 (s, 2H).

3-(Benzyloxy)-6-nitroquinazoline-2,4(1H,3H)-dione. Light yellow solid, 69% yield, mp: 269-271 °C. ¹H NMR (400 MHz, DMSO-*d*₆) δ 12.29 (s, 1H), 8.67 (d, *J* = 2.6 Hz, 1H), 8.50 (dd, *J* = 8.8, 2.7 Hz, 1H), 7.61 – 7.54 (m, 2H), 7.47 – 7.40 (m, 3H), 7.37 (d, *J* = 9.0 Hz, 1H), 5.13 (s, 2H).

4.1.3. General procedure for the synthesis of 6-amino-3-(benzyloxy)quinazoline-2,4(1H,3H)-dione or 7-amino-3-(benzyloxy)quinazoline-2,4(1H,3H)-dione (4)

A suspension of the nitro compound (1 mmol) and tin chloride dihydrate (4.8 eq) in ethanol (10 mL) was stirred at 80 °C for 1.5 h. Celite and solid NaHCO₃ (10 equiv) were added to the cooled solution followed by the dropwise addition of water until all acid was neutralized. The suspension was filtered, diluted with EtOAc, washed with brine, dried, filtered, evaporated, and flash chromatographed (EtOAc–petroleum ether) to provide the aniline.

7-Amino-3-(benzyloxy)quinazoline-2,4(1H,3H)-dione. Light yellow solid, 74% yield, ¹H NMR (400 MHz, DMSO-*d*₆) δ 11.22 (s, 1H), 7.59 (d, *J* = 8.7 Hz, 1H), 7.56 (dd, *J* = 7.7, 1.8 Hz, 2H), 7.45 – 7.36 (m, 3H), 6.42 (dd, *J* = 8.7, 2.0 Hz, 1H), 6.30 (s, 2H), 6.20 (d, *J* = 2.0 Hz, 1H), 5.03 (s, 2H).

6-Amino-3-(benzyloxy)quinazoline-2,4-(1*H*,3*H*)-dione. Light yellow solid, 37% yield, ¹H NMR (400 MHz, DMSO-*d*₆) δ 11.25 (s, 1H), 7.61 – 7.50 (m, 2H), 7.45 – 7.32 (m, 3H), 7.12 (d, *J* = 2.2 Hz, 1H), 6.98 – 6.87 (m, 2H), 5.28 (s, 2H), 5.07 (s, 2H).

4.1.4. General procedure for the synthesis of **5**

To a solution of **7a** (1 mmol) in pyridine (8 mL) were added corresponding substituted benzyl chloride or benzyl sulfonyl chloride (1.5 mmol). After the mixture was stirred for 3 h (monitored by TLC), it was acidified to pH 7 with 1N hydrochloric acid solution. The resulting precipitate was filtered and recrystallized.

N-(3-(Benzyloxy)-2,4-dioxo-1,2,3,4-tetrahydroquinazolin-7-yl)benzamide (**5A-1**). White solid, 49% yield; ¹H NMR (400 MHz, DMSO-*d*₆) δ 11.69 (s, 1H), 10.68 (s, 1H), 7.96 (dd, *J* = 16.1, 8.4 Hz, 4H), 7.63 (t, *J* = 7.3 Hz, 1H), 7.57 (dd, *J* = 8.2, 4.7 Hz, 5H), 7.46 – 7.38 (m, 3H), 5.10 (s, 2H). ESI-MS: *m/z* 386.17 [M-H]⁻. C₂₂H₁₇N₃O₄ (387.40)

N-(3-(Benzyloxy)-2,4-dioxo-1,2,3,4-tetrahydroquinazolin-7-yl)-4-fluorobenzamide (**5A-2**). White solid, 53% yield; ¹H NMR (400 MHz, DMSO-*d*₆) δ 11.71 (s, 1H), 10.69 (s, 1H), 8.07 (dd, *J* = 8.6, 5.6 Hz, 2H), 7.97 – 7.90 (m, 2H), 7.62 – 7.53 (m, 3H), 7.47 – 7.38 (m, 5H), 5.10 (s, 2H). C₂₂H₁₆FN₃O₄ (405.39)

N-(3-(Benzyloxy)-2,4-dioxo-1,2,3,4-tetrahydroquinazolin-7-yl)-4-methylbenzamide (**5A-3**). White solid, 69% yield; ¹H NMR (400 MHz, DMSO-*d*₆) δ 11.69 (s, 1H), 10.59 (s, 1H), 7.98 – 7.85 (m, 4H), 7.58 (td, *J* = 9.5, 8.8, 5.1 Hz, 3H), 7.46 – 7.35 (m, 5H), 5.10 (s, 2H), 2.41 (s, 3H). ESI-MS: *m/z* 400.17 [M-H]⁻. C₂₂H₁₉N₃O₄ (401.42)

N-(3-(Benzyloxy)-2,4-dioxo-1,2,3,4-tetrahydroquinazolin-7-yl)-4-(trifluoromethyl)benzamide (**5A-4**). White solid, 51% yield; ¹H NMR (400 MHz, DMSO-*d*₆) δ 11.74 (s, 1H), 10.88 (s, 1H), 8.31 (s, 1H), 8.29 (d, *J* = 8.0 Hz, 1H), 8.04 – 7.92 (m, 3H), 7.82 (t, *J* = 7.8 Hz, 1H), 7.58 (ddd, *J* = 8.7, 4.5, 2.0 Hz, 3H), 7.46 – 7.39 (m, 3H), 5.11 (s, 2H). ESI-MS: *m/z* 454.20 [M-H]⁻. C₂₃H₁₆F₃N₃O₄ (455.39)

N-(3-(Benzyloxy)-2,4-dioxo-1,2,3,4-tetrahydroquinazolin-7-yl)-3-fluorobenzamide (**5A-5**). White solid, 44% yield; ¹H NMR (400 MHz, DMSO-*d*₆) δ 11.72 (s, 1H), 10.73 (s, 1H), 7.95 (d, *J* = 8.8 Hz, 2H), 7.82 (t, *J* = 10.7 Hz, 2H), 7.60 (ddt, *J* = 14.1, 8.3, 4.8 Hz, 4H), 7.45 (qd, *J* = 15.2, 13.3, 8.2 Hz, 4H), 5.11 (s, 2H). ESI-MS: *m/z* 404.13 [M-H]⁻. C₂₂H₁₆FN₃O₄ (405.39)

N-(3-(Benzyloxy)-2,4-dioxo-1,2,3,4-tetrahydroquinazolin-7-yl)-3-(trifluoromethyl)benzenesulfonamide (**5A-6**). White solid, 61% yield; ¹H NMR (400 MHz, DMSO-*d*₆) δ 11.60 (s, 1H), 11.25 (s, 1H), 8.15 (d, *J* = 6.8 Hz, 2H), 8.09 (d, *J* = 7.8 Hz, 1H), 7.86 (dd, *J* = 19.3, 8.4 Hz, 2H), 7.54 (dd, *J* = 7.3, 1.8 Hz, 2H), 7.45 – 7.36 (m, 3H), 7.08 (d, *J* = 1.8 Hz, 1H), 6.95 (dd, *J* = 8.7, 1.9 Hz, 1H), 5.04 (s, 2H). ESI-MS: *m/z* 490.09 [M-H]⁻. C₂₂H₁₆F₃N₃O₅S (491.44)

N-(3-(Benzyloxy)-2,4-dioxo-1,2,3,4-tetrahydroquinazolin-7-yl)naphthalene-2-sulfonamide (**5A-7**). White solid, 77% yield; ¹H NMR (400 MHz, DMSO-*d*₆) δ 11.56 (s, 1H), 11.21 (s, 1H), 8.60 (d, *J* = 1.9 Hz, 1H), 8.15 (dd, *J* = 14.7, 8.0 Hz, 2H), 8.06 – 7.99 (m, 1H), 7.83 (dd, *J* = 8.7, 1.9 Hz, 1H), 7.79 (d, *J* = 8.7 Hz, 1H), 7.71 (tt, *J* = 7.0, 5.4 Hz, 2H), 7.55 – 7.48 (m, 2H), 7.43 – 7.34 (m, 3H), 7.10 (d, *J* = 2.0 Hz, 1H), 6.97 (dd, *J* = 8.7, 2.1 Hz, 1H), 4.99 (s, 2H). C₂₂H₁₉N₃O₅S (473.50)

N-(3-(Benzyloxy)-2,4-dioxo-1,2,3,4-tetrahydroquinazolin-7-yl)-2,4,6-trimethylbenzenesulfonamide (**5A-8**). White solid, 51% yield; ¹H NMR (400 MHz, DMSO-*d*₆) δ 11.66 (s, 1H), 11.00 (s, 1H), 7.80 (d, *J* = 8.6 Hz, 1H), 7.58 – 7.48 (m, 2H), 7.43 – 7.34 (m, 3H), 7.05 (s, 2H), 6.84 (dd, *J* = 8.7, 2.0 Hz, 1H), 6.79 (d, *J* = 1.9 Hz, 1H), 5.02 (s, 2H), 2.63 (s, 6H), 2.23 (s, 3H). ESI-MS: *m/z* 464.15 [M-H]⁻. C₂₄H₂₃N₃O₅S (465.52)

4-(Tert-butyl)-*N*-(3-(benzyloxy)-2,4-dioxo-1,2,3,4-tetrahydroquinazolin-7-yl)benzenesulfonamide (**5A-9**). White solid, 49% yield; ESI-MS: *m/z* 478.11[M-H]⁻. C₂₅H₂₅N₃O₅S (479.55)

4-Fluoro-*N*-(3-(benzyloxy)-2,4-dioxo-1,2,3,4-tetrahydroquinazolin-7-yl)benzenesulfonamide (**5A-10**). White solid, 33% yield; ESI-MS: *m/z* 440.11[M-H]⁻. C₂₁H₁₆FN₃O₅S (441.43)

N-(3-(Benzyloxy)-2,4-dioxo-1,2,3,4-tetrahydroquinazolin-7-yl)-[1,1'-biphenyl]-4-sulfonamide (**5A-11**). White solid, 81% yield; ¹H NMR (400 MHz, DMSO-*d*₆) δ 11.59 (s, 1H), 11.15 (s, 1H), 7.96 (d, *J* = 8.5 Hz, 2H), 7.90 (d, *J* = 8.5 Hz, 2H), 7.83 (d, *J* = 8.7 Hz, 1H), 7.74 – 7.68 (m, 2H), 7.56 – 7.46 (m, 4H), 7.46 – 7.37 (m, 4H), 7.12 (d, *J* = 2.0 Hz, 1H), 6.97 (dd, *J* = 8.7, 2.0 Hz, 1H), 5.03 (s, 2H). ESI-MS: *m/z* 498.15 [M-H]⁻. C₂₇H₂₁N₃O₅S (499.54)

N-(3-(Benzyloxy)-2,4-dioxo-1,2,3,4-tetrahydroquinazolin-7-yl)-3-methylbenzenesulfonamide (**5A-12**). White solid, 76% yield; ¹H NMR (400 MHz, DMSO-*d*₆) δ 11.58 (s, 1H), 11.06 (s, 1H), 7.81 (d, *J* = 8.7 Hz, 1H), 7.72 (s, 1H), 7.67 (dt, *J* = 5.9, 2.8 Hz, 1H), 7.57 – 7.52 (m, 2H), 7.50 – 7.45 (m, 2H), 7.43 – 7.36 (m, 3H), 7.06 (d, *J* = 2.0 Hz, 1H), 6.93 (dd, *J* = 8.7, 2.1 Hz, 1H), 5.03 (s, 2H), 2.38 (s, 3H). ESI-MS: *m/z* 436.13 [M-H]⁻. C₂₂H₁₉N₃O₅S (437.47)

N-(3-(Benzyloxy)-2,4-dioxo-1,2,3,4-tetrahydroquinazolin-6-yl)-2-fluorobenzamide (**5B-1**).

White solid, 55% yield; ESI-MS: *m/z* 404.14 [M-H]⁻. C₂₂H₁₆FN₃O₄ (405.39)

N-(3-(Benzyloxy)-2,4-dioxo-1,2,3,4-tetrahydroquinazolin-6-yl)benzenesulfonamide (**5B-2**).

White solid, 63% yield; ESI-MS: *m/z* 422.08 [M-H]⁻. C₂₁H₁₇N₃O₅S (423.44)

N-(3-(Benzyloxy)-2,4-dioxo-1,2,3,4-tetrahydroquinazolin-6-yl)-4-fluorobenzenesulfonamide (**5B-3**). White solid, 59% yield; ESI-MS: *m/z* 440.12 [M-H]⁻. C₂₁H₁₆FN₃O₅S (441.43)

N-(3-(Benzyloxy)-2,4-dioxo-1,2,3,4-tetrahydroquinazolin-6-yl)naphthalene-2-sulfonamide (**5B-4**). White solid, 44% yield; ¹H NMR (400 MHz, DMSO-*d*₆) δ 11.56 (s, 1H), 10.55 (s, 1H), 8.41 (s, 1H), 8.12 (t, *J* = 8.2 Hz, 2H), 8.01 (d, *J* = 8.0 Hz, 1H), 7.78 (dd, *J* = 8.7, 1.7 Hz, 1H), 7.75 – 7.61 (m, 3H), 7.52 (dd, *J* = 7.2, 2.0 Hz, 2H), 7.48 (dd, *J* = 8.8, 2.5 Hz, 1H), 7.39 (dq, *J* = 7.0, 2.9, 2.2 Hz, 3H), 7.08 (d, *J* = 8.8 Hz, 1H), 5.02 (s, 2H). C₂₅H₁₉FN₃O₅S (473.50)

N-(3-(Benzyloxy)-2,4-dioxo-1,2,3,4-tetrahydroquinazolin-6-yl)-3-(trifluoromethyl)benzenesulfonamide (**5B-5**). White solid, 62% yield; ¹H NMR (400 MHz, DMSO-*d*₆) δ 8.05 (d, *J* = 7.9 Hz, 1H), 8.02 (s, 1H), 7.99 (d, *J* = 8.0 Hz, 1H), 7.82 (t, *J* = 7.8 Hz, 1H), 7.60 (d, *J* = 2.5 Hz, 1H), 7.57 – 7.52 (m, 2H), 7.46 – 7.37 (m, 4H), 7.13 (d, *J* = 8.8 Hz, 1H), 5.05 (s, 2H). C₂₂H₁₆F₃N₃O₅S (491.44)

4.1.5. General procedure for the synthesis of 6

Intermediate 5 was dissolved in MeOH (5 mL) and CH₂Cl₂ (5 mL) and the solution was degassed and stirred at room temperature under H₂ over 10% Pd/C (10% w/w, 2 h-12h). The mixture was filtered. The filtrate was concentrated and the resulting residue was recrystallized in MeOH and CH₂Cl₂.

N-(3-hydroxy-2,4-dioxo-1,2,3,4-tetrahydroquinazolin-7-yl)benzamide (**I-1**). Light yellow solid, 34% yield, mp: 155-157 °C; ¹H NMR (400 MHz, DMSO-*d*₆) δ 11.59 (s, 1H), 10.67 (s, 1H), 10.51 (s, 1H), 8.01 – 7.94 (m, 3H), 7.91 (d, *J* = 8.7 Hz, 1H), 7.63 (t, *J* = 7.3 Hz, 1H), 7.59 – 7.51 (m, 3H); ¹³C NMR (100 MHz, DMSO-*d*₆) δ 166.68, 159.47, 149.46, 145.18, 139.70, 134.91, 132.46, 128.91, 128.35, 128.28, 115.41, 109.96, 105.35. ESI-MS: *m/z* 296.20 [M-H]⁻. C₁₅H₁₁N₃O₄ (297.27)

4-Fluoro-*N*-(3-hydroxy-2,4-dioxo-1,2,3,4-tetrahydroquinazolin-7-yl)benzamide (**I-2**). White solid, 19% yield, mp > 300 °C; ¹H NMR (400 MHz, DMSO-*d*₆) δ 11.10 (s, 1H), 10.67 (s, 1H), 8.14 – 8.01 (m, 2H), 7.97 – 7.79 (m, 2H), 7.54 (d, *J* = 8.8 Hz, 1H), 7.39 (t, *J* = 8.6 Hz, 2H); ¹³C NMR (100 MHz, DMSO-*d*₆) δ 165.54, 164.77 (*J* = 247 Hz), 159.48, 149.46, 145.11, 139.68, 131.31,

131.23 ($2 \times C$, $J = 9$ Hz), 128.25, 115.87 ($2 \times C$, $J = 22$ Hz), 115.46, 109.99, 105.42. ESI-MS: m/z 314.18 $[M-H]^-$. $C_{15}H_{10}FN_3O_4$ (315.26)

N-(3-Hydroxy-2,4-dioxo-1,2,3,4-tetrahydroquinazolin-7-yl)-4-methylbenzamide (**I-3**). White solid, 55% yield, mp: 227-229 °C; 1H NMR (400 MHz, DMSO- d_6) δ 11.57 (s, 1H), 10.55 (s, 1H), 10.49 (s, 1H), 7.97 – 7.86 (m, 4H), 7.54 (d, $J = 8.6$ Hz, 1H), 7.36 (d, $J = 7.9$ Hz, 2H), 2.40 (s, 3H); ^{13}C NMR (100 MHz, DMSO- d_6) δ 166.44, 159.48, 149.48, 145.25, 142.60, 139.71, 131.99, 129.43, 128.39, 128.24, 115.39, 109.86, 105.31, 21.52. ESI-MS: m/z 310.27 $[M-H]^-$; m/z 334.12 $[M+Na]^+$. $C_{16}H_{13}N_3O_4$ (311.29)

N-(3-Hydroxy-2,4-dioxo-1,2,3,4-tetrahydroquinazolin-7-yl)-4-(trifluoromethyl)benzamide (**I-4**). White solid, 25% yield, mp: 275-277 °C; 1H NMR (400 MHz, DMSO- d_6) δ 10.85 (s, 1H), 8.35 – 8.21 (m, 2H), 8.01 (d, $J = 7.8$ Hz, 1H), 7.93 (m, 2H), 7.81 (t, $J = 7.8$ Hz, 1H), 7.54 (dd, $J = 8.7$, 1.9 Hz, 1H). ^{13}C NMR (100 MHz, DMSO- d_6) δ 165.21, 159.45, 149.46, 144.79, 139.69, 135.80, 129.65 ($2 \times C$, $J = 227$ Hz), 129.24 ($J = 227$ Hz), 128.99 ($J = 4$ Hz), 124.93 ($2 \times C$, $J = 4$ Hz), 123.04, 115.48, 110.29, 105.59. ESI-MS: m/z 364.30 $[M-H]^-$. $C_{16}H_{10}F_3N_3O_4$ (365.26)

3-Fluoro-*N*-(3-hydroxy-2,4-dioxo-1,2,3,4-tetrahydroquinazolin-7-yl)benzamide (**I-5**). Gray solid, 28% yield, mp > 300 °C; 1H NMR (400 MHz, DMSO- d_6) δ 11.60 (s, 1H), 10.70 (s, 1H), 10.52 (s, 1H), 7.92 (d, $J = 7.4$ Hz, 2H), 7.82 (t, $J = 10.8$ Hz, 2H), 7.62 (dd, $J = 13.9$, 7.8 Hz, 1H), 7.57 – 7.46 (m, 2H). ESI-MS: m/z 314.27 $[M-H]^-$; m/z 316.17 $[M+H]^+$. $C_{15}H_{10}FN_3O_4$ (315.26)

N-(3-Hydroxy-2,4-dioxo-1,2,3,4-tetrahydroquinazolin-7-yl)-3-(trifluoromethyl)benzenesulfonamide (**I-6**). White solid, 33% yield, mp: 198-200 °C; 1H NMR (400 MHz, DMSO- d_6) δ 11.46 (s, 1H), 11.19 (s, 1H), 10.46 (s, 1H), 8.13 (d, $J = 5.9$ Hz, 2H), 8.06 (d, $J = 7.9$ Hz, 1H), 7.85 (t, $J = 8.1$ Hz, 1H), 7.78 (d, $J = 8.7$ Hz, 1H), 7.03 (d, $J = 2.0$ Hz, 1H), 6.90 (dd, $J = 8.7$, 2.0 Hz, 1H). ^{13}C NMR (100 MHz, DMSO- d_6) δ 159.29, 149.22, 140.97, 139.91, 131.66, 131.22, 130.58, 130.26, 129.20, 123.71, 122.37, 114.13, 110.01, 103.70. ESI-MS: m/z 400.20 $[M-H]^-$. $C_{15}H_{10}F_3N_3O_5S$ (401.32)

N-(3-Hydroxy-2,4-dioxo-1,2,3,4-tetrahydroquinazolin-7-yl)naphthalene-2-sulfonamide (**I-7**). White solid, 36% yield, mp: 245-247 °C; 1H NMR (400 MHz, DMSO- d_6) δ 11.41 (s, 1H), 11.16 (s, 1H), 10.41 (s, 1H), 8.57 (d, $J = 1.9$ Hz, 1H), 8.20 – 8.07 (m, 2H), 8.06 – 7.99 (m, 1H), 7.82 (dd, $J = 8.7$, 1.9 Hz, 1H), 7.77 – 7.64 (m, 3H), 7.05 (d, $J = 2.0$ Hz, 1H), 6.93 (dd, $J = 8.7$, 2.0 Hz, 1H). ^{13}C NMR (100 MHz, DMSO- d_6) δ 159.31, 149.23, 139.85, 136.87, 134.82, 131.95, 130.14,

129.75 , 129.61 , 128.95 , 128.73 , 128.34 , 128.28 , 122.40 , 113.86 , 109.39 , 103.12, 99.99 .

ESI-MS: m/z 382.20 [M-H]⁻. C₁₈H₁₃N₃O₅S (383.38)

N-(3-Hydroxy-2,4-dioxo-1,2,3,4-tetrahydroquinazolin-7-yl)-2,4,6-trimethylbenzenesulfonamide (**I-8**). White solid, 29% yield, mp: 278-280 °C; ¹H NMR (400 MHz, DMSO-*d*₆) δ 11.54 (s, 1H), 10.97 (s, 1H), 10.44 (s, 1H), 7.76 (d, *J* = 8.6 Hz, 1H), 7.03 (s, 2H), 6.81 (dd, *J* = 8.7, 2.1 Hz, 1H), 6.77 (d, *J* = 2.0 Hz, 1H), 2.62 (s, 6H), 2.23 (s, 3H); ¹³C NMR (100 MHz, DMSO-*d*₆) δ 159.32, 149.33, 144.47, 142.87, 139.89, 139.28 (2×C), 133.94, 132.37 (2×C), 129.10, 112.98, 109.14, 101.83, 22.90 (2×C), 20.86. ESI-MS: m/z 374.29 [M-H]⁻. C₁₇H₁₇N₃O₅S (375.40)

4-(Tert-butyl)-*N*-(3-hydroxy-2,4-dioxo-1,2,3,4-tetrahydroquinazolin-7-yl)benzenesulfonamide (**I-9**). White solid, 46% yield, mp: 153-155 °C; ¹H NMR (400 MHz, DMSO-*d*₆) δ 11.45 (s, 1H), 11.02 (s, 1H), 10.46 (s, 1H), 7.80 (d, *J* = 8.5 Hz, 2H), 7.77 (d, *J* = 8.8 Hz, 1H), 7.61 (d, *J* = 8.5 Hz, 2H), 7.08 – 7.05 (d, *J* = 1.7 Hz, 1H), 6.91 (dd, *J* = 8.7, 1.7 Hz, 1H), 1.26 (s, 9H); ¹³C NMR (100 MHz, DMSO-*d*₆) δ 159.34, 156.72, 149.25, 144.53, 139.92, 137.14, 129.06, 127.11 (2×C), 126.77 (2×C), 113.54, 109.45, 102.85, 35.38 (3×C), 31.16. ESI-MS: m/z 388.30 [M-H]⁻. C₁₈H₁₉N₃O₅S (389.43)

4-Fluoro-*N*-(3-hydroxy-2,4-dioxo-1,2,3,4-tetrahydroquinazolin-7-yl)benzenesulfonamide (**I-10**). White solid, 29% yield, mp: 267-269 °C; ¹H NMR (400 MHz, DMSO-*d*₆) δ 11.47 (s, 1H), 11.06 (s, 1H), 10.48 (s, 1H), 7.98 – 7.88 (m, 2H), 7.80 (d, *J* = 8.7 Hz, 1H), 7.46 (t, *J* = 8.8 Hz, 2H), 7.04 (d, *J* = 2.0 Hz, 1H), 6.92 (dd, *J* = 8.6, 2.0 Hz, 1H); ¹³C NMR (100 MHz, DMSO-*d*₆) δ 166.28, 163.77, 159.31, 149.21, 143.79, 139.89, 135.90 (*J* = 3 Hz), 130.37 (2×C, *J* = 10 Hz), 129.16, 117.22 (2×C, *J* = 22 Hz), 111.85 (*J* = 378 Hz), 103.38. ESI-MS: m/z 350.21 [M-H]⁻. C₁₄H₁₀FN₃O₅S (351.31)

N-(3-Hydroxy-2,4-dioxo-1,2,3,4-tetrahydroquinazolin-7-yl)-[1,1'-biphenyl]-4-sulfonamide (**I-11**). White solid, 31% yield, mp > 300 °C; ¹H NMR (400 MHz, DMSO-*d*₆) δ 11.45 (s, 1H), 11.23 – 10.98 (m, 1H), 10.45 (s, 1H), 7.94 (d, *J* = 8.3 Hz, 2H), 7.88 (d, *J* = 8.4 Hz, 2H), 7.78 (d, *J* = 8.7 Hz, 1H), 7.71 (d, *J* = 7.3 Hz, 2H), 7.49 (dd, *J* = 8.2, 6.6 Hz, 2H), 7.43 (t, *J* = 7.2 Hz, 1H), 7.08 (d, *J* = 1.9 Hz, 1H), 6.93 (dd, *J* = 8.8, 2.0 Hz, 1H); ¹³C NMR (100 MHz, DMSO-*d*₆) δ 159.35, 149.25, 145.13, 144.47, 139.93, 138.66, 138.60, 129.58 (2×C), 129.12, 129.09, 128.06 (2×C), 127.92 (2×C), 127.57 (2×C), 113.75, 109.59, 103.14. ESI-MS: m/z 408.20 [M-H]⁻. C₂₀H₁₅N₃O₅S (409.42)

N-(3-Hydroxy-2,4-dioxo-1,2,3,4-tetrahydroquinazolin-7-yl)-3-methylbenzenesulfonamide (**I-12**). White solid, 41% yield; ¹H NMR (400 MHz, DMSO-*d*₆) δ 11.45 (s, 1H), 11.00 (s, 1H), 10.45

(s, 1H), 7.77 (d, $J = 8.7$ Hz, 1H), 7.70 (s, 1H), 7.67 – 7.61 (m, 1H), 7.53 – 7.42 (m, 2H), 7.02 (d, $J = 1.7$ Hz, 1H), 6.89 (dd, $J = 8.7, 1.8$ Hz, 1H), 2.37 (s, 3H); ^{13}C NMR (100 MHz, DMSO- d_6) δ 159.33, 149.25, 144.20, 139.87, 139.67, 139.61, 134.45, 129.77, 129.06, 127.47, 124.42, 113.61, 109.61, 102.99, 21.31. ESI-MS: m/z 346.19 [M-H] $^-$. $\text{C}_{15}\text{H}_{13}\text{N}_3\text{O}_5\text{S}$ (347.35)

2-Fluoro-*N*-(3-hydroxy-2,4-dioxo-1,2,3,4-tetrahydroquinazolin-6-yl)benzamide (**II-1**). White solid, 18% yield, mp: 291-293 °C; ^1H NMR (400 MHz, DMSO- d_6) δ 11.56 (s, 1H), 10.61 (s, 2H), 8.43 (d, $J = 2.2$ Hz, 1H), 7.92 (dd, $J = 8.8, 2.3$ Hz, 1H), 7.69 (t, $J = 7.4$ Hz, 1H), 7.60 (q, $J = 6.0$ Hz, 1H), 7.36 (q, $J = 9.3, 7.5$ Hz, 2H), 7.20 (d, $J = 8.8$ Hz, 1H); ^{13}C NMR (100 MHz, DMSO- d_6) δ 163.20, 159.70, 159.35 ($J = 248$ Hz), 158.11, 149.02, 135.04, 134.27, 133.14 ($J = 8$ Hz), 130.41, 130.38, 127.44, 125.09 ($J = 2$ Hz), 125.05, 117.53, 116.67 ($J = 22$ Hz), 116.31, 114.67. ESI-MS: m/z 314.17 [M-H] $^-$. $\text{C}_{15}\text{H}_{10}\text{FN}_3\text{O}_4$ (315.26)

N-(3-Hydroxy-2,4-dioxo-1,2,3,4-tetrahydroquinazolin-6-yl)benzenesulfonamide (**II-2**). White solid, 26% yield, mp: 212-214 °C; ^1H NMR (400 MHz, DMSO- d_6) δ 11.50 (s, 1H), 10.56 (s, 1H), 10.38 (s, 1H), 7.71 (d, $J = 7.4$ Hz, 2H), 7.63 – 7.52 (m, 4H), 7.41 (dd, $J = 8.8, 2.4$ Hz, 1H), 7.09 (d, $J = 8.8$ Hz, 1H); ^{13}C NMR (100 MHz, DMSO- d_6) δ 159.36, 148.87, 139.50, 135.70, 133.49, 132.80, 129.78 ($2 \times \text{C}$), 128.87, 127.10 ($2 \times \text{C}$), 118.88, 116.94, 114.96. ESI-MS: m/z 332.08 [M-H] $^-$. $\text{C}_{14}\text{H}_{11}\text{N}_3\text{O}_5\text{S}$ (333.32)

4-Fluoro-*N*-(3-hydroxy-2,4-dioxo-1,2,3,4-tetrahydroquinazolin-6-yl)benzenesulfonamide (**II-3**). White solid, 28% yield, mp: 141-144 °C; ^1H NMR (400 MHz, DMSO- d_6) δ 11.46 (s, 1H), 10.57 (s, 2H), 7.77 (dd, $J = 8.6, 5.1$ Hz, 2H), 7.58 (d, $J = 2.4$ Hz, 1H), 7.45 – 7.34 (m, 3H), 7.11 (d, $J = 8.8$ Hz, 1H); ^{13}C NMR (100 MHz, DMSO- d_6) δ 166.02, 163.51, 159.36, 148.88, 135.92 ($J = 3$ Hz), 135.81, 132.73, 130.20 ($2 \times \text{C}$, $J = 9$ Hz), 129.13, 119.18, 116.99 ($2 \times \text{C}$, $J = 23$ Hz), 116.00 ($J = 199$ Hz). ESI-MS: m/z 350.13 [M-H] $^-$. $\text{C}_{14}\text{H}_{10}\text{FN}_3\text{O}_5\text{S}$ (351.31)

N-(3-Hydroxy-2,4-dioxo-1,2,3,4-tetrahydroquinazolin-6-yl)naphthalene-2-sulfonamide (**II-4**). White solid, 24% yield, mp: 194-195 °C; ^1H NMR (400 MHz, DMSO- d_6) δ 11.38 (s, 1H), 10.51 (s, 2H), 8.38 (d, $J = 1.8$ Hz, 1H), 8.09 (dd, $J = 11.0, 8.4$ Hz, 2H), 7.99 (d, $J = 8.0$ Hz, 1H), 7.75 (dd, $J = 8.7, 1.9$ Hz, 1H), 7.67 (dt, $J = 11.9, 7.3$ Hz, 2H), 7.61 (d, $J = 2.4$ Hz, 1H), 7.41 (dd, $J = 8.7, 2.6$ Hz, 1H), 7.05 (d, $J = 8.8$ Hz, 1H); ^{13}C NMR (100 MHz, DMSO- d_6) δ 159.36, 148.85, 136.92, 135.46, 134.66, 133.29, 131.99, 129.90, 129.67, 129.41, 128.82, 128.33, 128.28, 128.15, 122.51, 118.75, 116.88, 114.96. ESI-MS: m/z 382.13 [M-H] $^-$. $\text{C}_{18}\text{H}_{13}\text{N}_3\text{O}_5\text{S}$ (383.38)

N-(3-Hydroxy-2,4-dioxo-1,2,3,4-tetrahydroquinazolin-6-yl)-3-(trifluoromethyl)benzenesulfonamide (**II-5**). White solid, 33% yield, mp: 207-209 °C; ¹H NMR (400 MHz, DMSO-*d*₆) δ 11.53 (s, 1H), 10.57 (s, 1H), 10.52 (s, 1H), 8.09 – 7.93 (m, 3H), 7.80 (t, *J* = 7.8 Hz, 1H), 7.56 (d, *J* = 2.5 Hz, 1H), 7.41 (dd, *J* = 8.7, 2.5 Hz, 1H), 7.12 (d, *J* = 8.8 Hz, 1H); ¹³C NMR (100 MHz, DMSO-*d*₆) δ 159.28, 148.87, 140.60, 136.16, 132.15, 131.51, 131.19, 130.47, 130.28, 130.24, 130.14, 129.46, 123.64 (*J* = 4 Hz), 121.06 (*J* = 266 Hz), 115.03. ESI-MS: *m/z* 400.14 [M-H]⁻. C₁₅H₁₀F₃N₃O₅S (401.32)

4.2. *In vitro* anti-HIV assay

By using the MTT method described previously [24, 25], the synthesized compounds were evaluated for their activity against WT HIV-1 [26] (strain IIIB), and HIV-2 [27] (strain ROD) in MT-4 cells. First, stock solutions (10× final concentration) of test compounds were added at 25 μL volumes to two series of triplicate wells to allow simultaneous evaluation of their effects on mock and HIV-infected cells. Serial five-fold dilutions of the test compounds were made directly in flat-bottomed 96-well microtiter trays, including untreated control HIV-1 and mock-infected cells for each sample, using a Biomek 3000 robot (Beckman instruments, Fullerton, CA). HIV-1 (IIIB), or HIV-2 (ROD) stocks (50 mL at 100-300 50% cell culture infectious doses (CCID₅₀)) or culture medium were added to either the mock or HIV-infected wells of the microtiter tray.

Mock-infected cells were used to evaluate the effect of test compounds on uninfected cells in order to assess their cytotoxicity. Exponentially growing MT-4 cells were centrifuged for 5 min at 1000 rpm and the supernatant was discarded. MT-4 cells were then resuspended at 6×10⁵ cells/mL, and 50 μL aliquots were transferred to the microtiter tray wells. Five days after infection the viability of mock-and HIV-infected cells was determined spectrophotometrically.

The MTT assay was based on the reduction of yellow colored 3(4,5-dimethylthiazol-2-yl)-2,5-diphenyltetrazolium bromide (MTT) (Acros Organics, Geel, Belgium) by mitochondrial dehydrogenase of metabolically active cells to a blue-purple formazan that can be measured spectrophotometrically. The absorbances were read in an eight-channel computer-controlled photometer (Multiscan Ascent Reader, Labsystems, Helsinki, Finland) at the wavelengths of 540 and 690 nm. All data were calculated using the median OD (optical density) value of two or three wells.

4.3. HIV-1 RNase H inhibition assay

Wild-type (WT) HIV-1 BH10 RT was expressed in *E. coli* and purified as previously described [28, 29]. The RT RNase H activity was determined with an RNA/DNA hybrid containing ³²P-labeled template RNA (31Trna, 5'-UUUUUUUUUAGGAUACAUAUGGUUAAAGUAU-3') and a DNA oligonucleotide 21P (5'-ATACTTTAACCATATGTATCC-3') [20]. RNase H cleavage assays were carried out at 37°C with 20-40 nM HIV-1 RT in 30 µl of 50 mM Tris-HCl (pH 8.0), 50 mM NaCl, 5 mM MgCl₂, 25 nM ³²P-labeled template-primer (31Trna/21P), and 5% dimethyl sulfoxide (DMSO). IC₅₀ values were determined from dose-response curves after calculating the amount of cleaved substrate in the absence of inhibitor (5% DMSO) or in the presence of the tested compounds at concentrations in the range of 0.2 to 100 µM [21].

4.4. HIV-1 IN strand transfer inhibition assays

WT HIV-1 IN was expressed in *E. coli* and purified as previously described [30], and the strand transfer inhibitory activity of tested compounds was determined as previously described [21, 31] using DNA complexes containing ³²P-labeled INT1ST (5'-ATGTGGAAAATCTCTAGCA-3') and non-labeled INT2 (5'-ACTGCTAGAGATTTTCCACAT-3'). The percentage inhibitory activity of tested compounds was determined at 1% DMSO in the absence of inhibitor and in the presence of raltegravir (MedChemExpress) or selected compounds at 1, 10 and 50 µM concentrations. For the determination of IC₅₀ values of raltegravir and compound II-4, strand transfer inhibitions were determined at additional concentrations in the range of 0.01 to 10 µM (i.e. 0.01, 0.05, 0.5 and 5 µM).

4.5. Cell permeability assays

Drug permeability was determined with the human colon epithelial cancer cell line, Caco-2, as previously described [21]. Caco-2 cell monolayers were used for measuring the rate of membrane transport for compound **II-4**, and expressed as apparent (P_{app}) permeability. Nadolol and metoprolol were used as controls in the assays.

The apparent permeability coefficient P_{app} (cm/s) was calculated using the equation: $P_{app} = (dCr/dt) \times V_r / (A \times C_0)$, where dCr/dt is the cumulative concentration of compound in the receiver chamber as a function of time (µM/s); V_r is the solution volume in the receiver chamber (0.075 mL on the apical side, 0.25 mL on the basolateral side); A is the surface area for the transport, i.e. 0.0804 cm² for the area of the monolayer; C_0 is the initial concentration in the donor chamber (µM). Analysis was carried out using Shimadzu LC 20-AD (Shimadzu, Japan), API 4000™ System (SCIEX, USA) and Apricot Designs Dual Arm (ADDA) (Apricot Designs, USA).

4.6. Computational methods and materials

Molecular modeling of molecule **II-4** was performed using the Tripos molecular modeling packages Sybyl-X 2.0. **II-4** was optimized for 2000-generations till the maximum derivative of energy became 0.005 kcal/(mol*Å) using the Tripos force field. The published three dimensional crystal structure of the PFV IN complex was obtained from the Protein Data Bank (PDB code: 3OYA). The published three dimensional crystal structure of the RNase H complex was downloaded from the Protein Data Bank (PDB code: 5J1E). The protein structure was prepared by using the Biopolymer application accompanying Sybyl. The ligand was extracted from the complexes, hydrogen atoms were added, side chain amides and side chains bumps were fixed, and charges and atom types were assigned according to AMBER 99. After the protomol was generated, the optimized **II-4** was docked into the binding pocket using the Surflex-Dock workflow of the SYBYL-X 2.0 software.

Conflict of interest

The authors declare no conflict of interest.

Acknowledgments

Financial support from the National Natural Science Foundation of China (NSFC No. 81273354), the Key Project of NSFC for International Cooperation (No. 81420108027), the Key Research and Development Project of Shandong Province (No. 2017CXGC1401), the Young Scholars Program of Shandong University (YSPSDU No. 2016WLJH32, to P. Z.), the Major Project of Science and Technology of Shandong Province (No. 2015ZDJS04001) is gratefully acknowledged. Work in Madrid was supported by grant BIO2016-76716-R (AEI/FEDER, UE) (Spanish Ministry of Economy, Industry and Competitiveness) and an institutional grant of Fundación Ramón Areces. The technical assistance of Mr. Kris Uyttersprot, and Mrs. Kristien Erven, for the HIV experiments is gratefully acknowledged.

References

- [1] UNAIDS. UNAIDS Data 2018 (2018), World Health Organization, Geneva, Switzerland.
- [2] P. Zhan, C. Pannecouque, E. De Clercq, X. Liu, Anti-HIV drug discovery and development: current innovations and future trends, *Journal of medicinal chemistry*, 59 (2016) 2849-2878.
- [3] L. Menéndez-Arias, Molecular basis of human immunodeficiency virus type 1 drug resistance: overview and recent developments, *Antiviral research*, 98 (2013) 93-120.
- [4] L. Menéndez-Arias, A. Sebastian-Martin, M. Álvarez, Viral reverse transcriptases, *Virus research*, 234 (2017) 153-176.

- [5] J.F. Davies, 2nd, Z. Hostomska, Z. Hostomsky, S.R. Jordan, D.A. Matthews, Crystal structure of the ribonuclease H domain of HIV-1 reverse transcriptase, *Science* (New York, N.Y.), 252 (1991) 88-95.
- [6] S. Hare, S.J. Smith, M. Metifiot, A. Jaxa-Chamiec, Y. Pommier, S.H. Hughes, P. Cherepanov, Structural and functional analyses of the second-generation integrase strand transfer inhibitor dolutegravir (S/GSK1349572), *Molecular pharmacology*, 80 (2011) 565-572.
- [7] S.X. Gu, P. Xue, X.L. Ju, Y.Y. Zhu, Advances in rationally designed dual inhibitors of HIV-1 reverse transcriptase and integrase, *Bioorganic & medicinal chemistry*, 24 (2016) 5007-5016.
- [8] L. Sun, P. Gao, G. Dong, X. Zhang, X. Cheng, X. Ding, X. Wang, D. Daelemans, E. De Clercq, C. Pannecouque, L. Menéndez-Arias, P. Zhan, X. Liu, 5-Hydroxypyrido[2,3-b]pyrazin-6(5H)-one derivatives as novel dual inhibitors of HIV-1 reverse transcriptase-associated ribonuclease H and integrase, *European journal of medicinal chemistry*, 155 (2018) 714-724.
- [9] K. Anstett, B. Brenner, T. Mesplede, M.A. Wainberg, HIV drug resistance against strand transfer integrase inhibitors. *Retrovirology*, 14 (2017) 36.
- [10] A. Markham, Bictegravir: first global approval, *Drugs*, 78 (2018) 601-606.
- [11] K.M. Brooks, E.M. Sherman, E.F. Egelund, A. Brotherton, S. Durham, M.E. Badowski, D.B. Cluck, Integrase inhibitors: After 10 years of experience, is the best yet to come? *Pharmacotherapy*, 39 (2019) 576-598.
- [12] B.A. Johns, T. Kawasuji, J.G. Weatherhead, T. Taishi, D.P. Temelkoff, H. Yoshida, T. Akiyama, Y. Taoda, H. Murai, R. Kiyama, M. Fuji, N. Tanimoto, J. Jeffrey, S.A. Foster, T. Yoshinaga, T. Seki, M. Kobayashi, A. Sato, M.N. Johnson, E.P. Garvey, T. Fujiwara, Carbamoyl pyridone HIV-1 integrase inhibitors 3. A diastereomeric approach to chiral nonracemic tricyclic ring systems and the discovery of dolutegravir (S/GSK1349572) and (S/GSK1265744). *Journal of medicinal chemistry*, 56(2013) 5901-5916.
- [13] A. Hombrouck, B. Van Remoortel, M. Michiels, W. Noppe, F. Christ, A. Eneroth, B.L. Sahlberg, K. Benkestock, L. Vrang, N.G. Johansson, M.L. Barreca, L. De Luca, S. Ferro, A. Chimirri, Z. Debyser, M. Witvrouw, Preclinical evaluation of 1H-benzylindole derivatives as novel human immunodeficiency virus integrase strand transfer inhibitors. *Antimicrobial agents and chemotherapy*, 52(2008) 2861-2869.
- [14] X. Wang, P. Gao, L. Menéndez-Arias, X. Liu, P. Zhan, Update on recent developments in small molecular HIV-1 RNase H inhibitors (2013-2016): opportunities and challenges. *Current medicinal chemistry*, 25 (2018) 1682-1702.
- [15] R. Costi, M. Métifiot, F. Esposito, G. Cuzzucoli Crucitti, L. Pescatori, A. Messori, L. Scipione, S. Tortorella, L. Zinzula, E. Novellino, Y. Pommier, E. Tramontano, C. Marchand, R. Di Santo, 6-(1-Benzyl-1H-pyrrol-2-yl)-2,4-dioxo-5-hexenoic acids as dual inhibitors of recombinant HIV-1 integrase and ribonuclease H, synthesized by a parallel synthesis approach, *Journal of medicinal chemistry*, 56(2013) 8588-8598.
- [16] T.A. Kirschberg, M. Balakrishnan, N.H. Squires, T. Barnes, K.M. Brendza, X. Chen, E.J. Eisenberg, W. Jin, N. Kutty, S. Leavitt, A. Licican, Q. Liu, X. Liu, J. Mak, J.K. Perry, M. Wang, W.J. Watkins, E.B. Lansdon, RNase H active site inhibitors of human immunodeficiency virus type 1 reverse transcriptase: design, biochemical activity, and structural information, *Journal of medicinal chemistry*, 52(2009) 5781-5784.
- [17] P. Zhan, X. Liu, Rationally designed multitarget anti-HIV agents, *Current medicinal chemistry*, 20(2013) 1743-1758.
- [18] L.N. Tumey, D. Bom, B. Huck, E. Gleason, J. Wang, D. Silver, K. Brunden, S. Boozer, S. Rundlett, B. Sherf, S. Murphy, T. Dent, C. Leventhal, A. Bailey, J. Harrington, Y.L. Bennani, The identification

and optimization of a N-hydroxy urea series of flap endonuclease 1 inhibitors, *Bioorganic medicinal chemistry letter*, 15 (2005) 277-281.

[19] J. Kankanala, K.A. Kirby, A.D. Huber, M.C. Casey, D.J. Wilson, S.G. Sarafianos, Z. Wang, Design, synthesis and biological evaluations of N-Hydroxy thienopyrimidine-2,4-diones as inhibitors of HIV reverse transcriptase-associated RNase H, *European journal of medicinal chemistry*, 141 (2017) 149-161.

[20] M. Álvarez, T. Matamoros, L. Menéndez-Arias, Increased thermostability and fidelity of DNA synthesis of wild-type and mutant HIV-1 group O reverse transcriptases, *Journal of molecular biology*, 392 (2009) 872-884.

[21] P. Gao, X. Wang, L. Sun, X. Cheng, V. Poongavanam, J. Kongsted, M. Álvarez, J. Luczkowiak, C. Pannecouque, E. De Clercq, K.H. Lee, C.H. Chen, H. Liu, L. Menéndez-Arias, X. Liu, P. Zhan, Design, synthesis, and biologic evaluation of novel galloyl derivatives as HIV-1 RNase H inhibitors. *Chemical biology & drug design*, 93 (2019) 582-589.

[22] S. Hare, A.M. Vos, R.F. Clayton, J.W. Thuring, M.D. Cummings, P. Cherepanov, Molecular mechanisms of retroviral integrase inhibition and the evolution of viral resistance, *Proceedings of the national academy of sciences of the united states of america*, 107 (2010) 20057-20062.

[23] S. Hare, S.S. Gupta, E. Valkov, A. Engelman, P. Cherepanov, Retroviral intasome assembly and inhibition of DNA strand transfer, *Nature*, 464 (2010) 232-236.

[24] R. Pauwels, J. Balzarini, M. Baba, R. Snoeck, D. Schols, P. Herdewijn, J. Desmyter, E. De Clercq, Rapid and automated tetrazolium-based colorimetric assay for the detection of anti-HIV compounds, *Journal of virological methods*, 20 (1988) 309-321.

[25] C. Pannecouque, D. Daelemans, E. De Clercq, Tetrazolium-based colorimetric assay for the detection of HIV replication inhibitors: revisited 20 years later, *Nature protocols*, 3 (2008) 427-434.

[26] M. Popovic, R.C. Gallo, Detection, isolation, and continuous production of cytopathic retroviruses (HTLV-III) from patients with AIDS and pre-AIDS, *Science*, 224 (1984) 497-500.

[27] F. Clavel, D. Guetard, F. Brunvezinet, S. Chamaret, M.A. Rey, M.O. Santosferreira, A.G. Laurent, C. Dauguet, C. Katlama, C. Rouzioux, Isolation of a new human retrovirus from west African patients with AIDS, *Science*, 233 (1986) 343-346.

[28] J. Boretto, S. Longhi, J.M. Navarro, B. Selmi, J. Sire, B. Canard, An integrated system to study multiply substituted human immunodeficiency virus type 1 reverse transcriptase, *Analytical biochemistry*, 292 (2001) 139-147.

[29] T. Matamoros, J. Deval, C. Guerreiro, L. Mulard, B. Canard, L. Menéndezarias, Suppression of multidrug-resistant HIV-1 reverse transcriptase primer unblocking activity by alpha-phosphate-modified thymidine analogues, *Journal of molecular biology*, 349 (2005) 451-463.

[30] G. Maertens, P. Cherepanov, W. Pluymers, K. Busschots, E. De Clercq, Z. Debyser, Y. Engelborghs, LEDGF/p75 is essential for nuclear and chromosomal targeting of HIV-1 integrase in human cells, *Journal of biological chemistry*, 278 (2003) 33528-33539.

[31] S.A. Chow, In vitro assays for activities of retroviral integrase, *Methods (San Diego, Calif.)*, 12 (1997) 306-317.

Design, synthesis and biological evaluation of 3-hydroxyquinazoline-2,4(1*H*,3*H*)-diones as dual inhibitors of HIV-1 reverse transcriptase-associated RNase H and integrase

Ping Gao^a, Xiqiang Cheng^a, Lin Sun^a, Shu Song^a, Mar Álvarez^b, Joanna Luczkowiak^b,
Christophe Pannecouque^c, Erik De Clercq^c, Luis Menéndez-Arias^{b,*}, Peng Zhan^{a,*}, Xinyong Liu^{a,*}

^aDepartment of Medicinal Chemistry, Key Laboratory of Chemical Biology, Ministry of Education, School of Pharmaceutical Sciences, Shandong University, Ji'nan, 250012

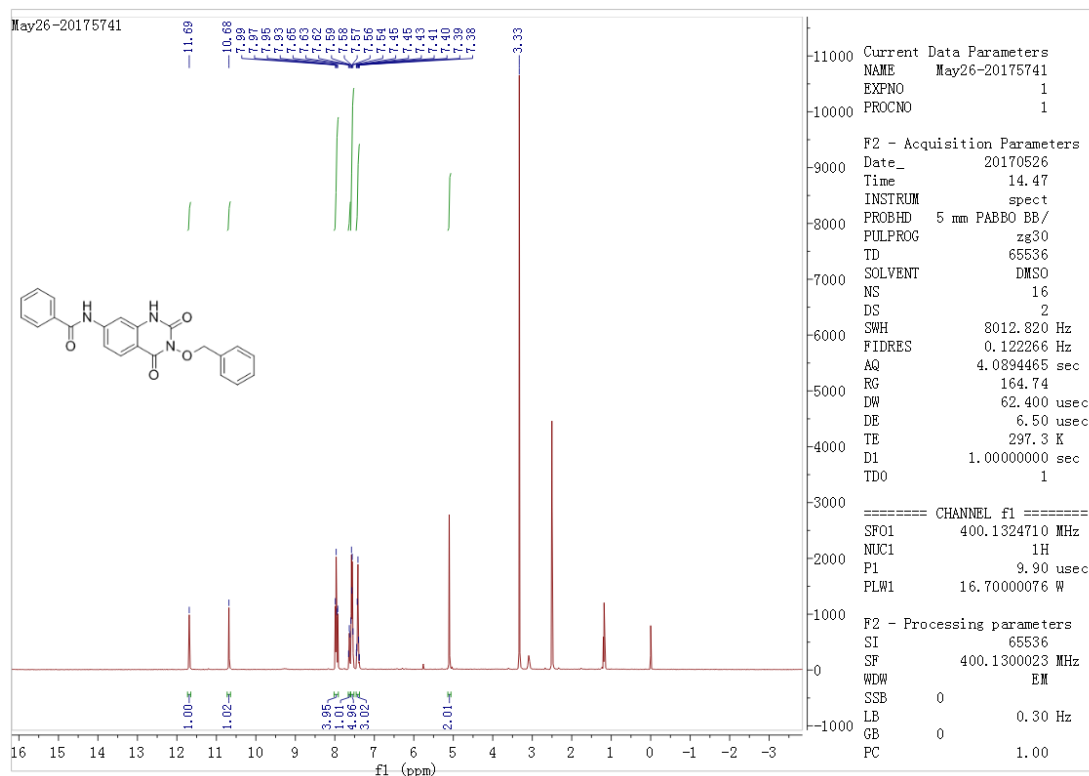
^bCentro de Biología Molecular “Severo Ochoa” (Consejo Superior de Investigaciones Científicas & Universidad Autónoma de Madrid), Madrid, Spain

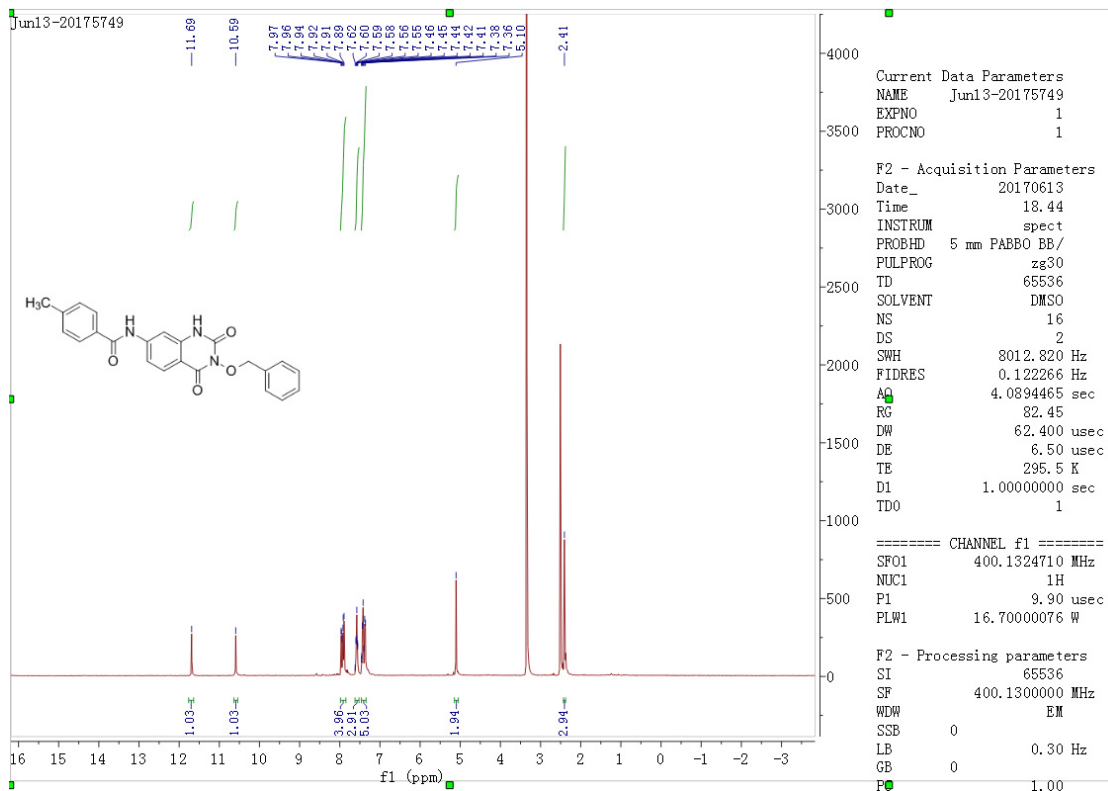
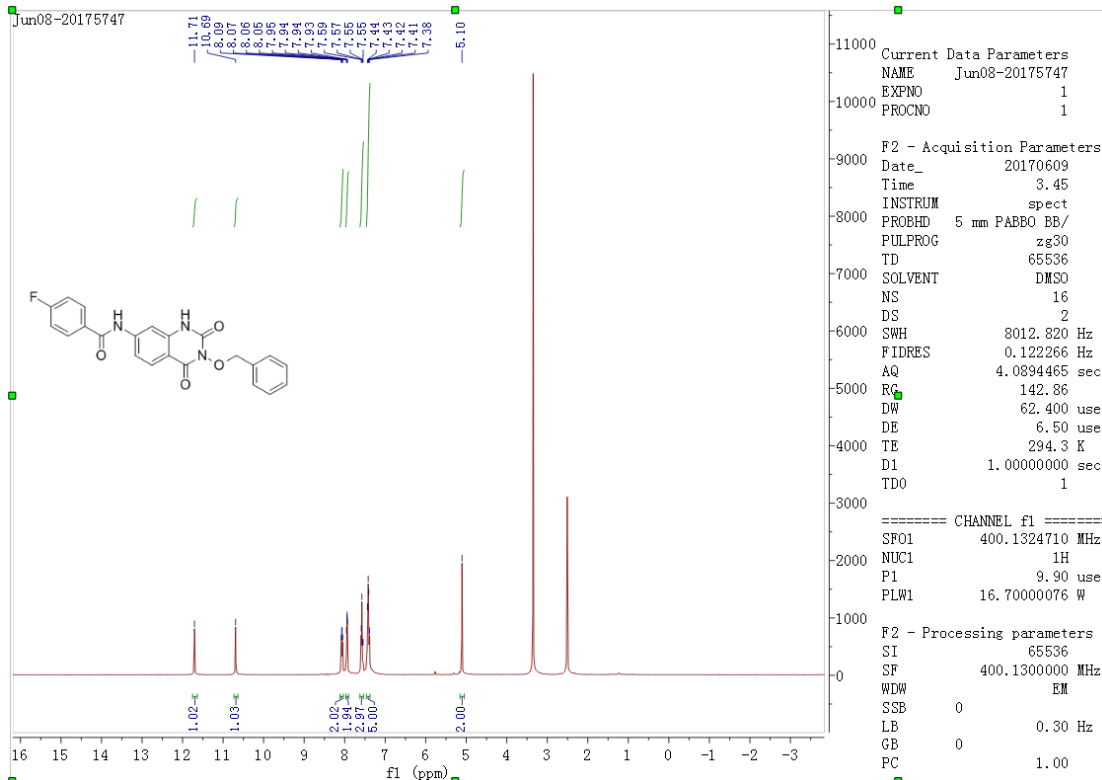
^cRega Institute for Medical Research, KU Leuven, Minderbroederstraat 10, B-3000 Leuven, Belgium

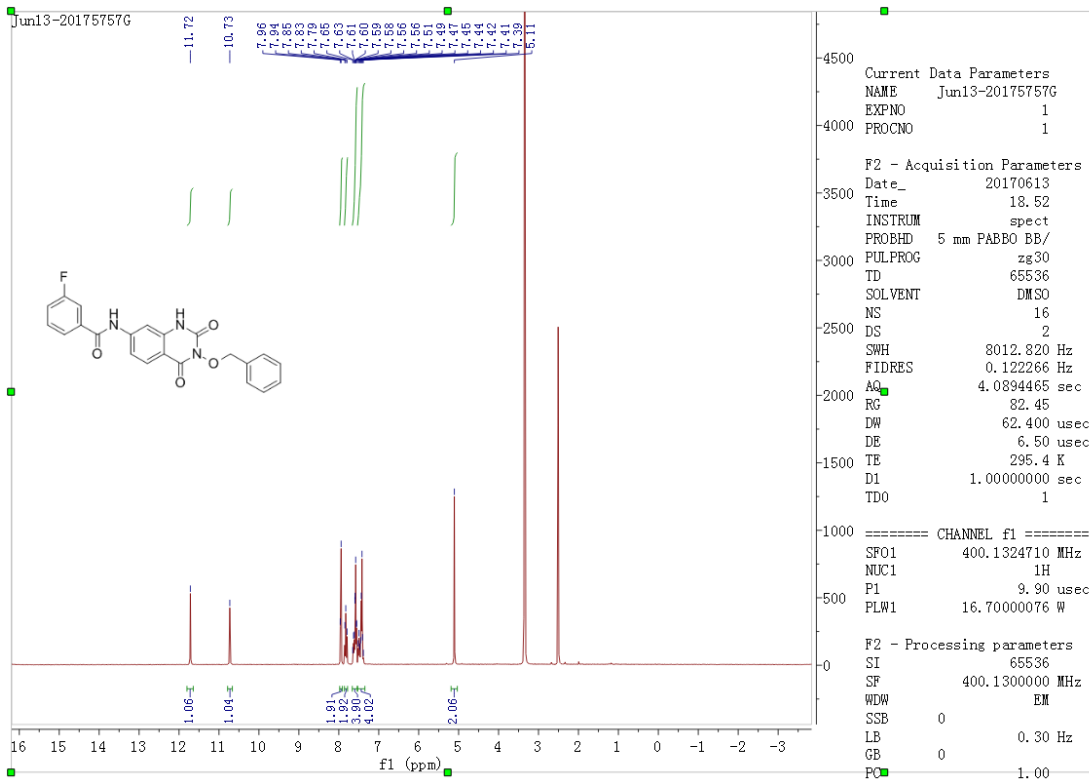
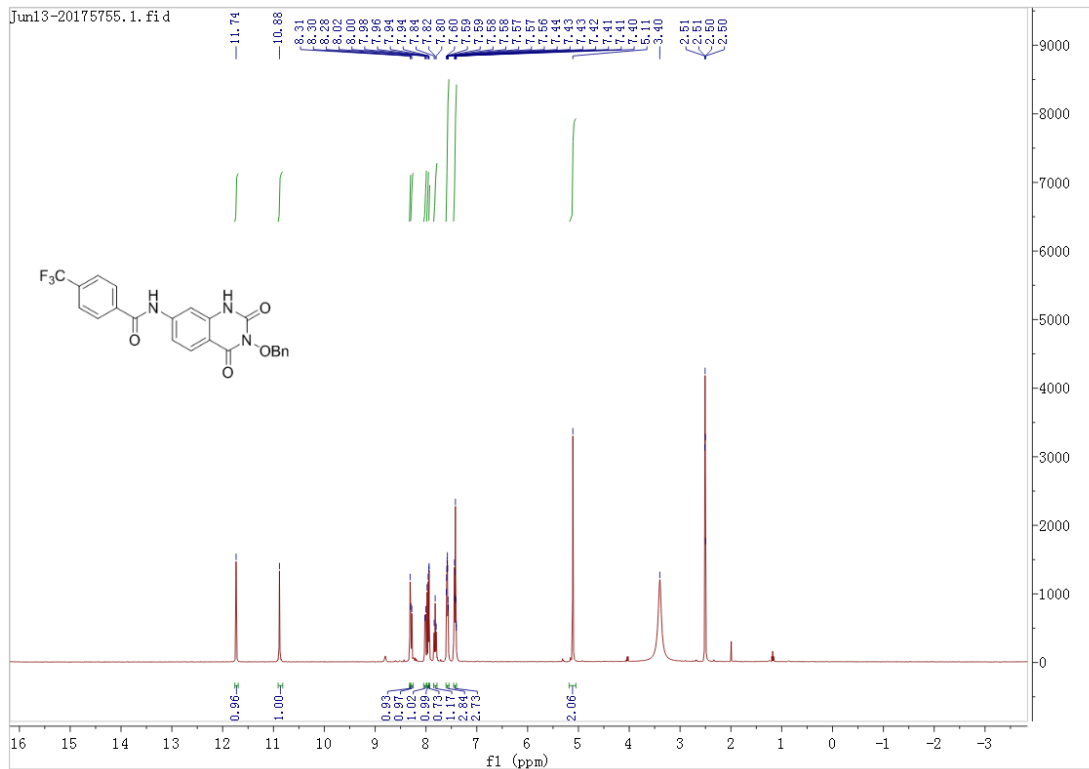
*E-mail: lmenendez@cbm.csic.es (Menéndez-Arias L.); zhanpeng1982@sdu.edu.cn (Zhan P.); xinyongl@sdu.edu.cn (Liu X.Y.).

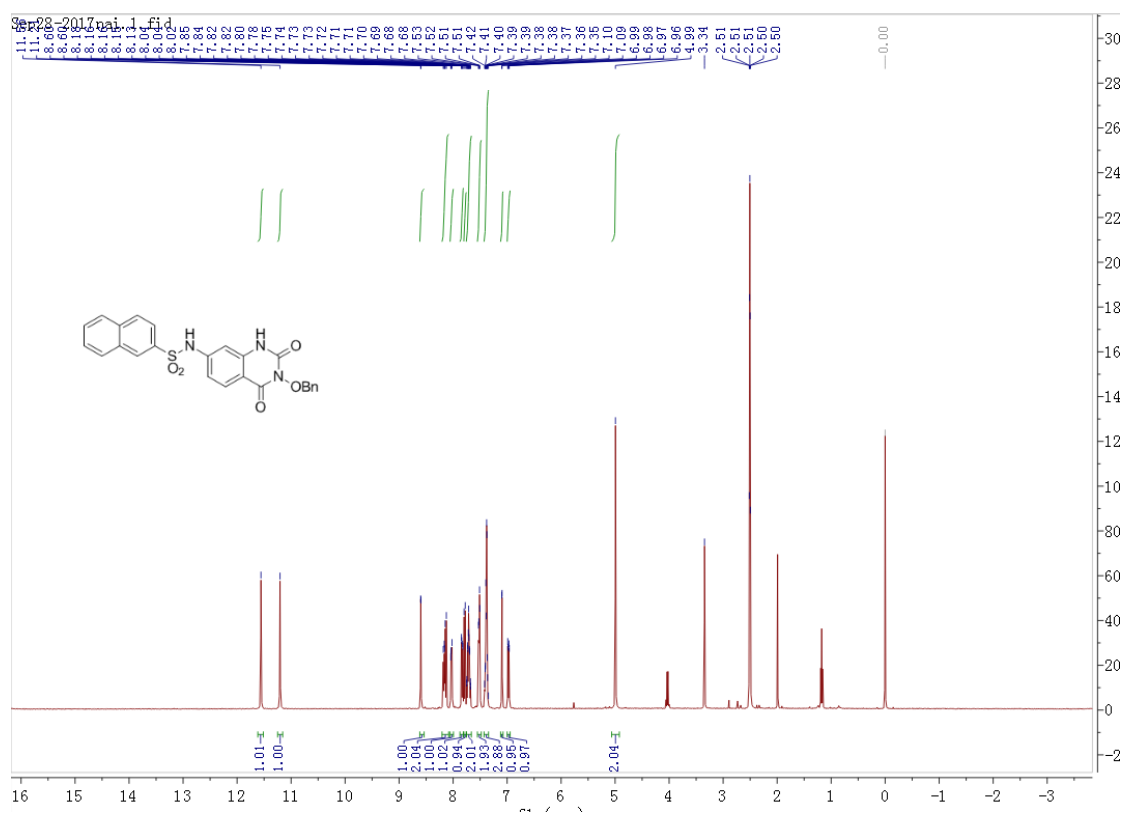
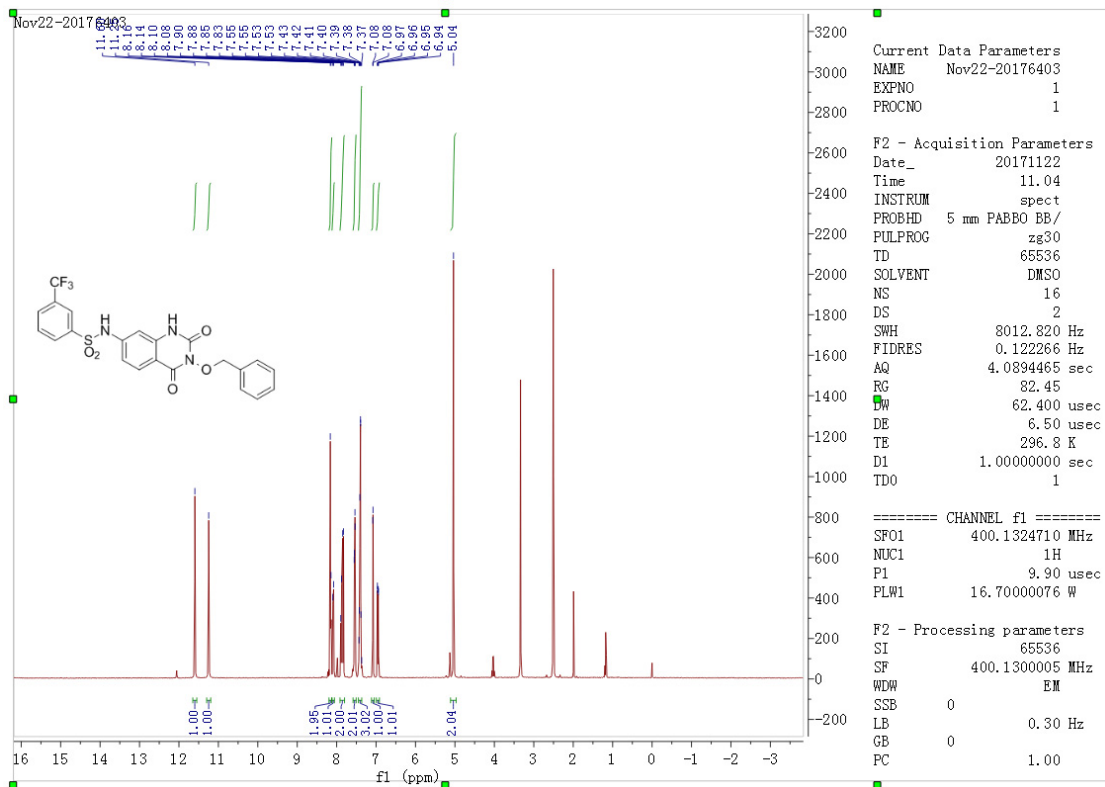
Supporting Information:

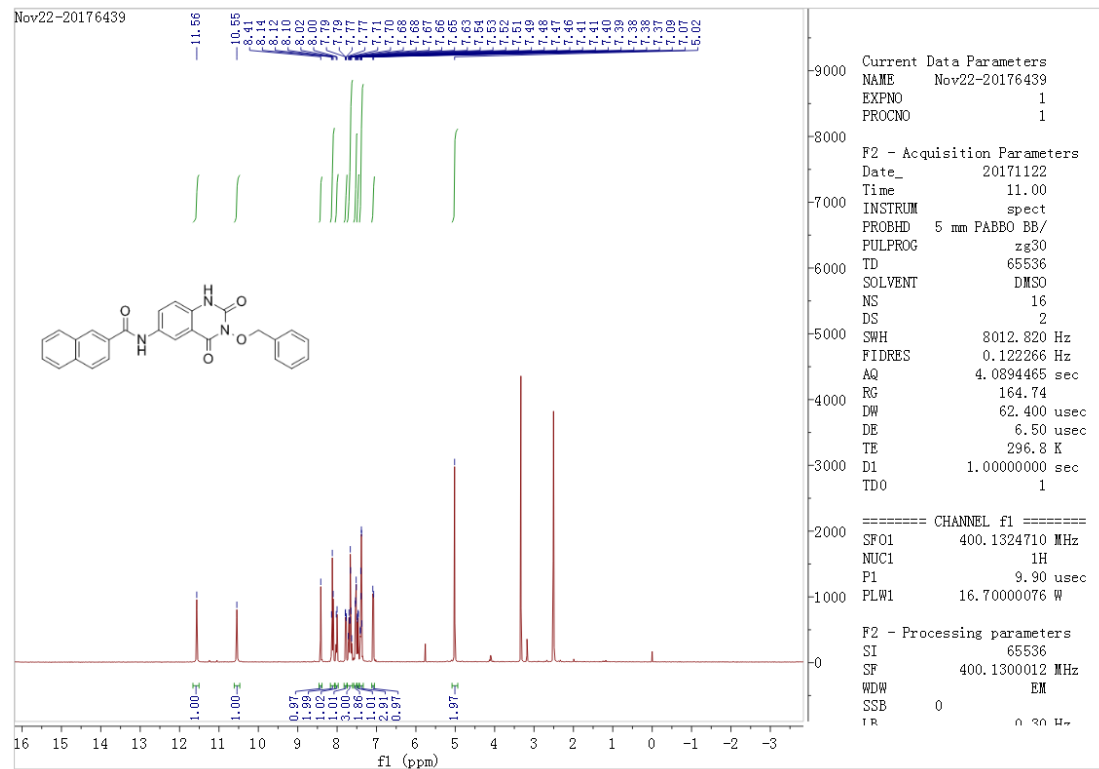
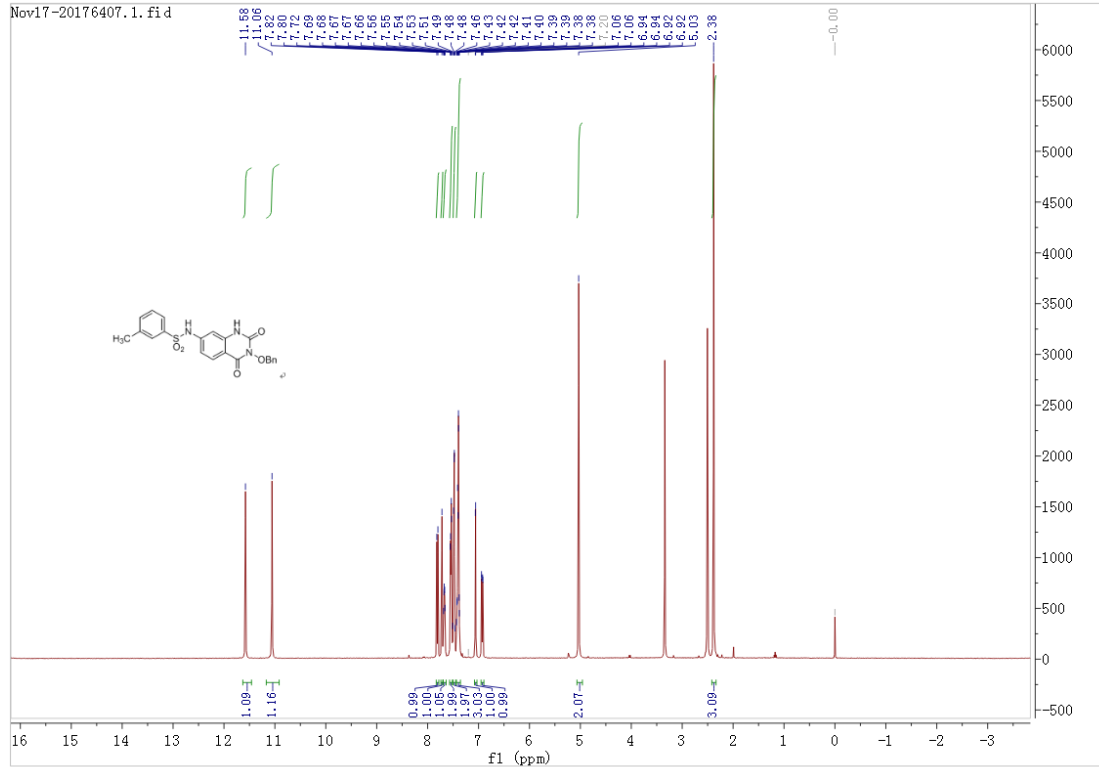
¹H NMR and ¹³C NMR spectra of representative compound:

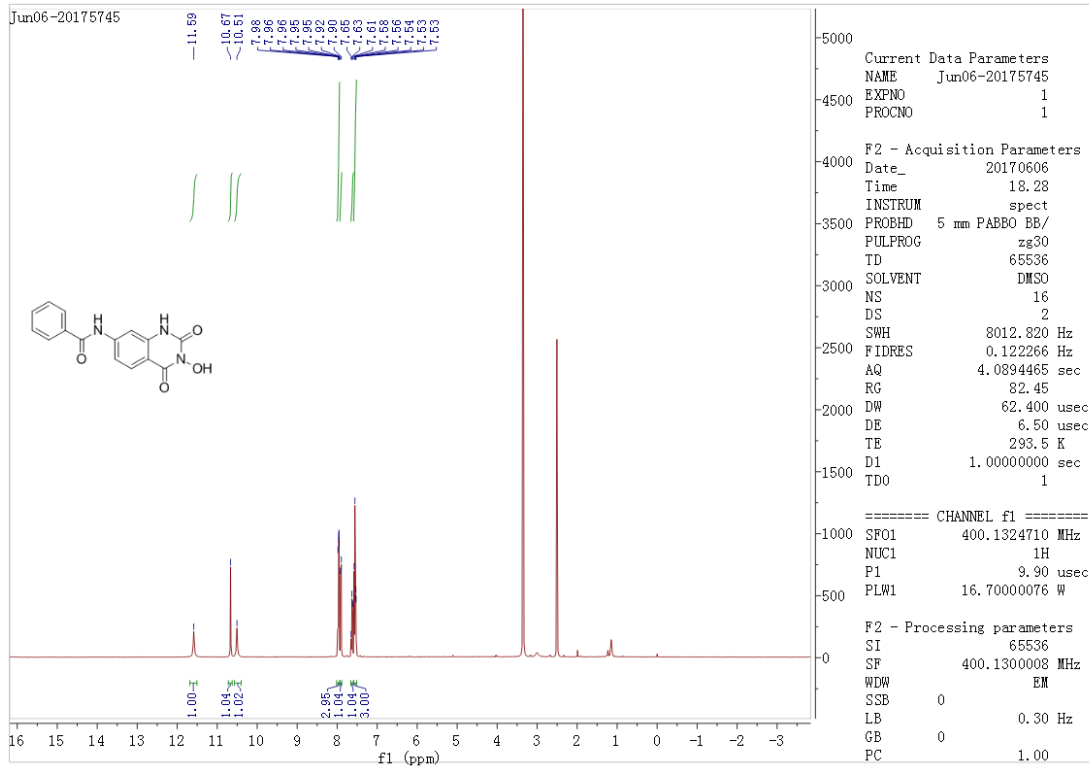
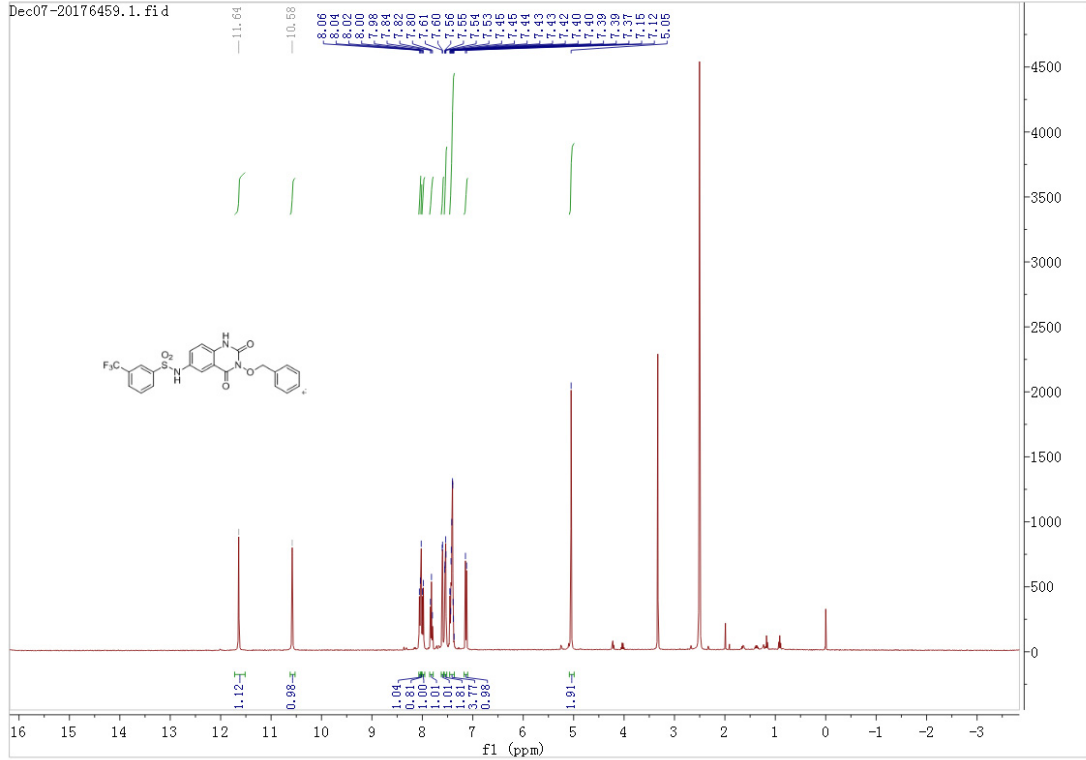




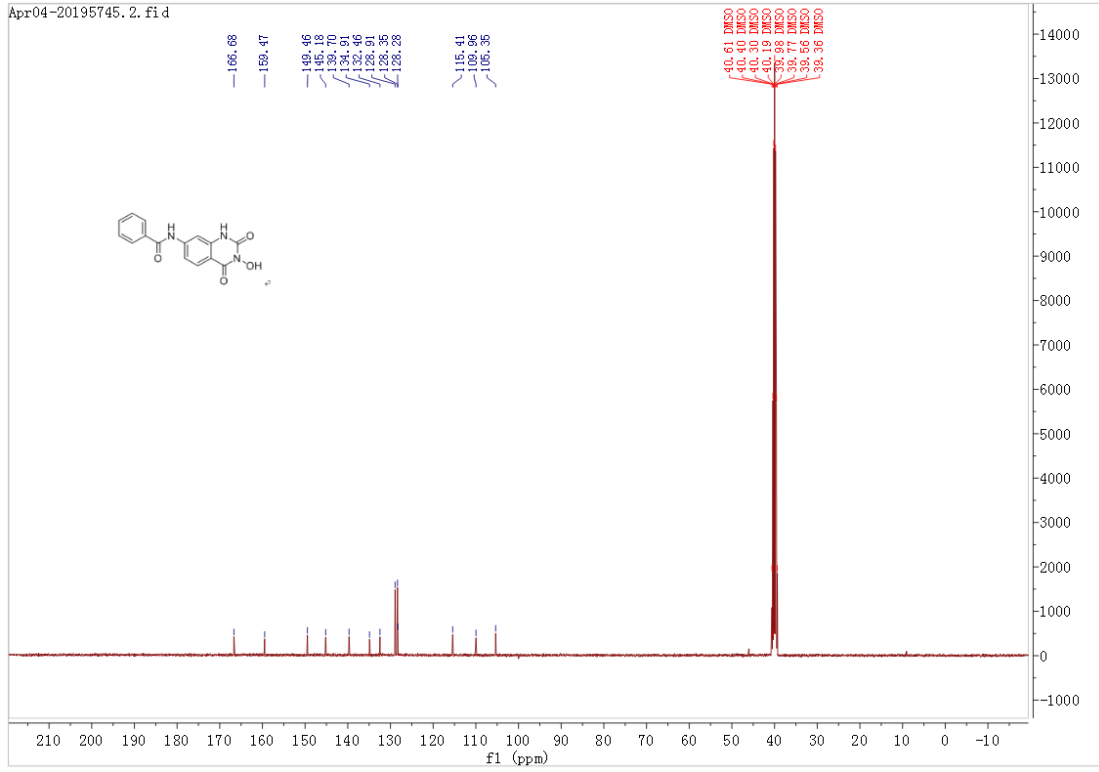




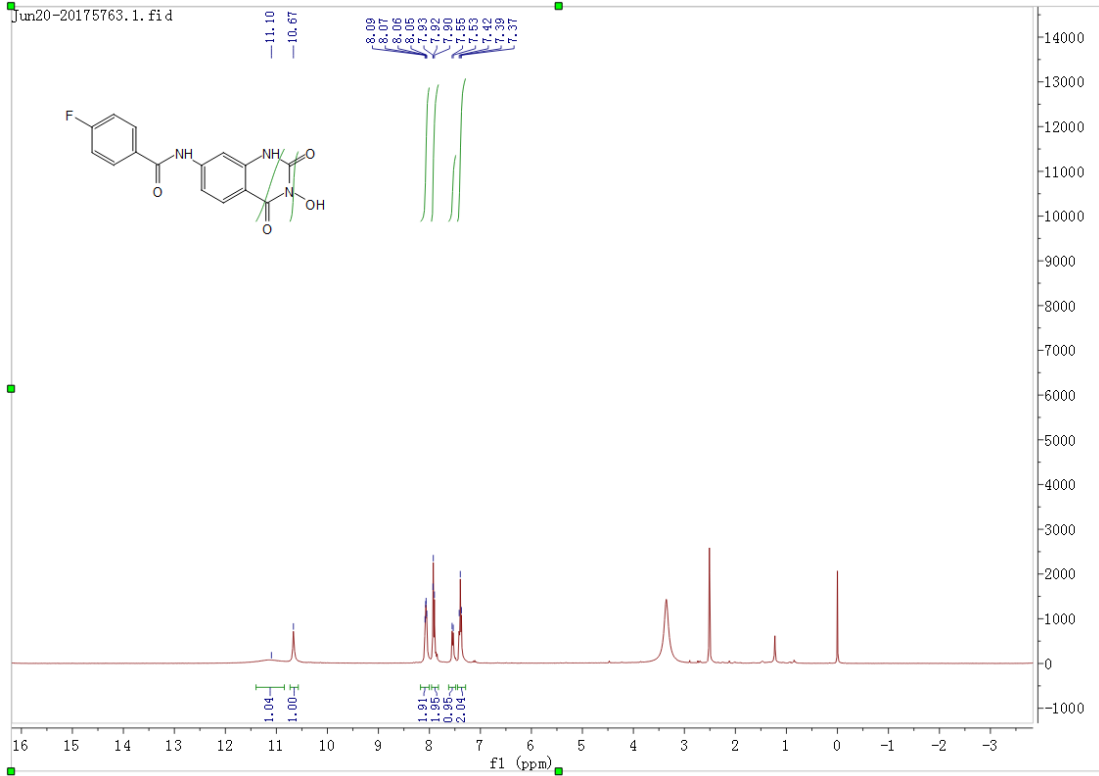


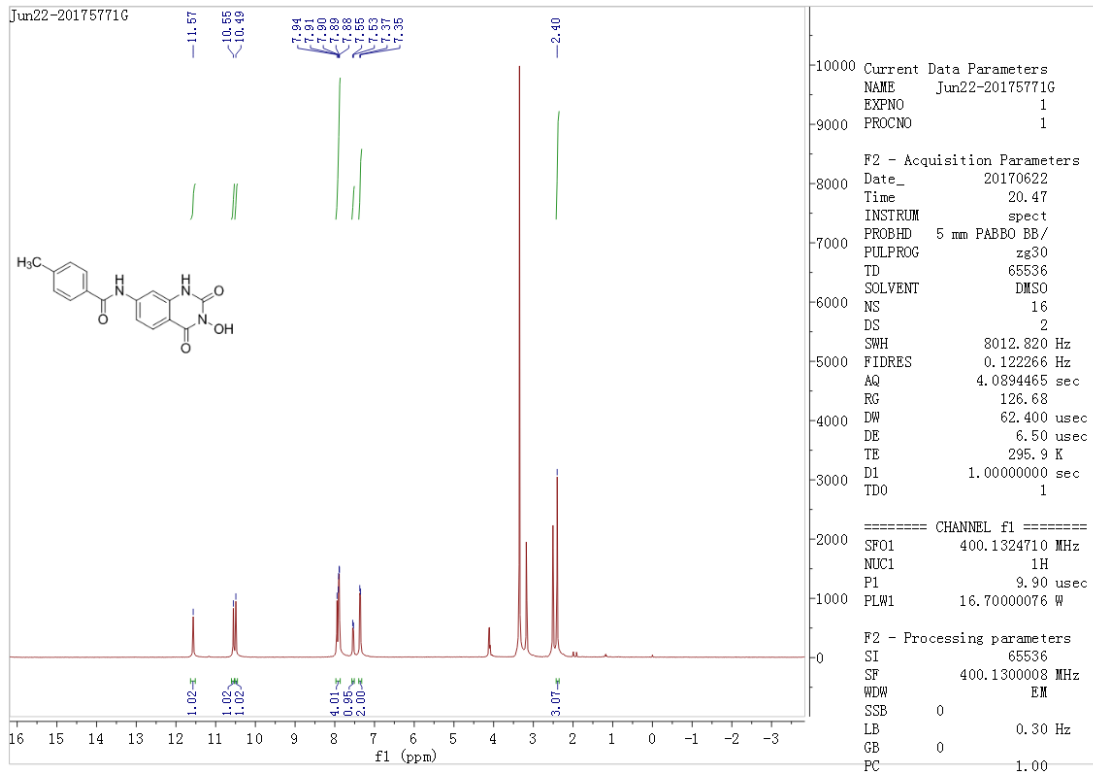
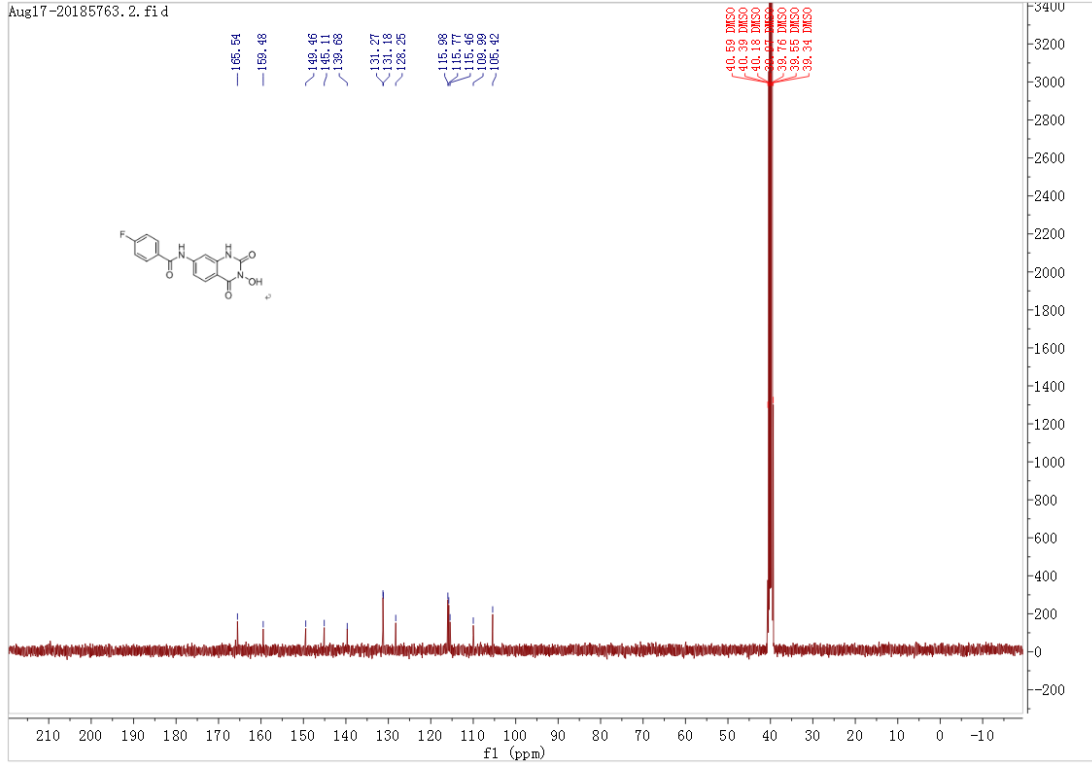


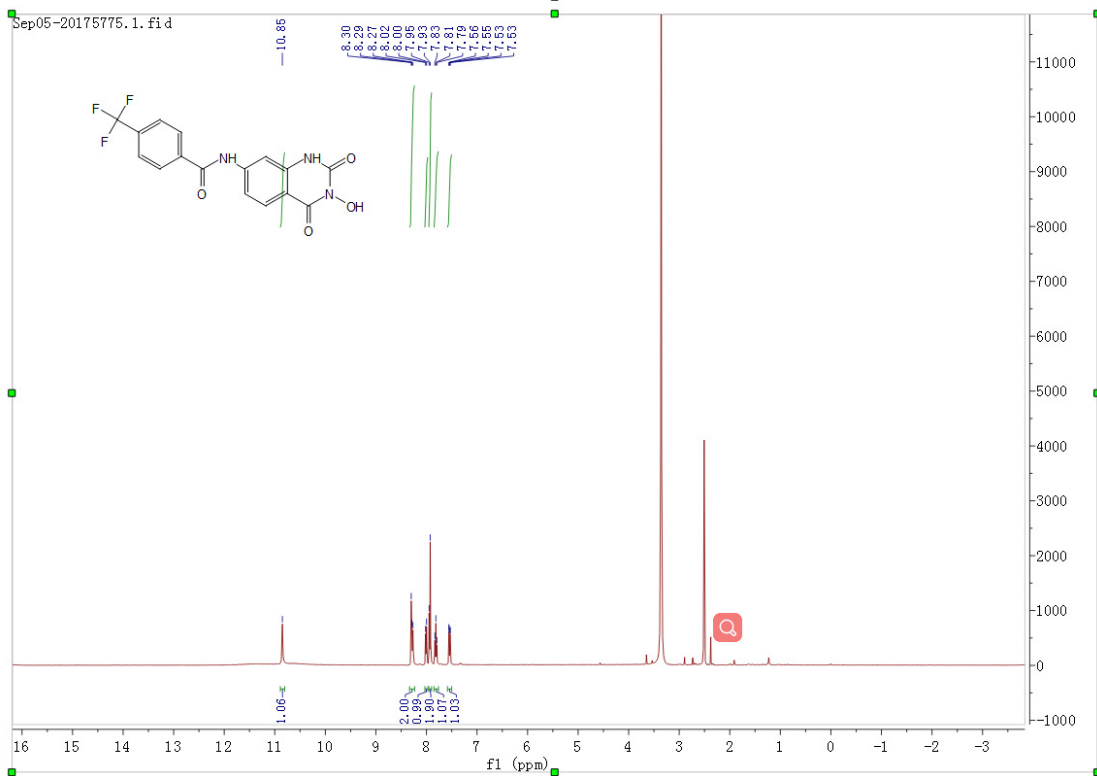
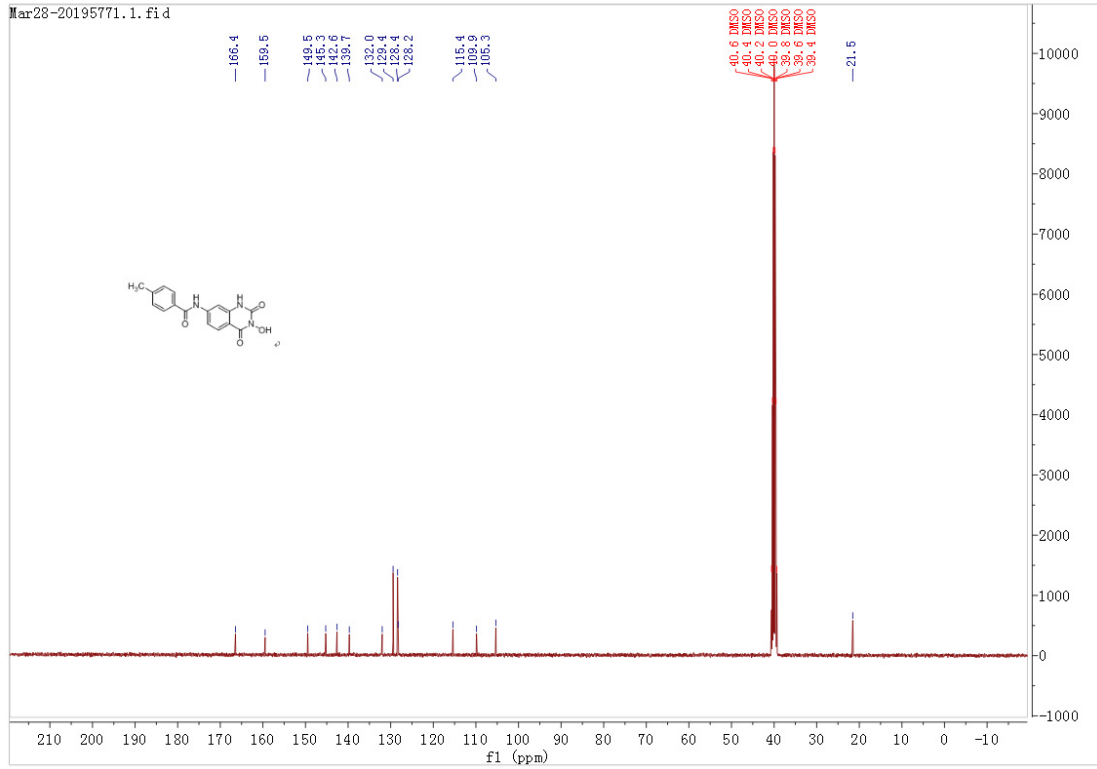
Apr04-20195745.2.f1 d



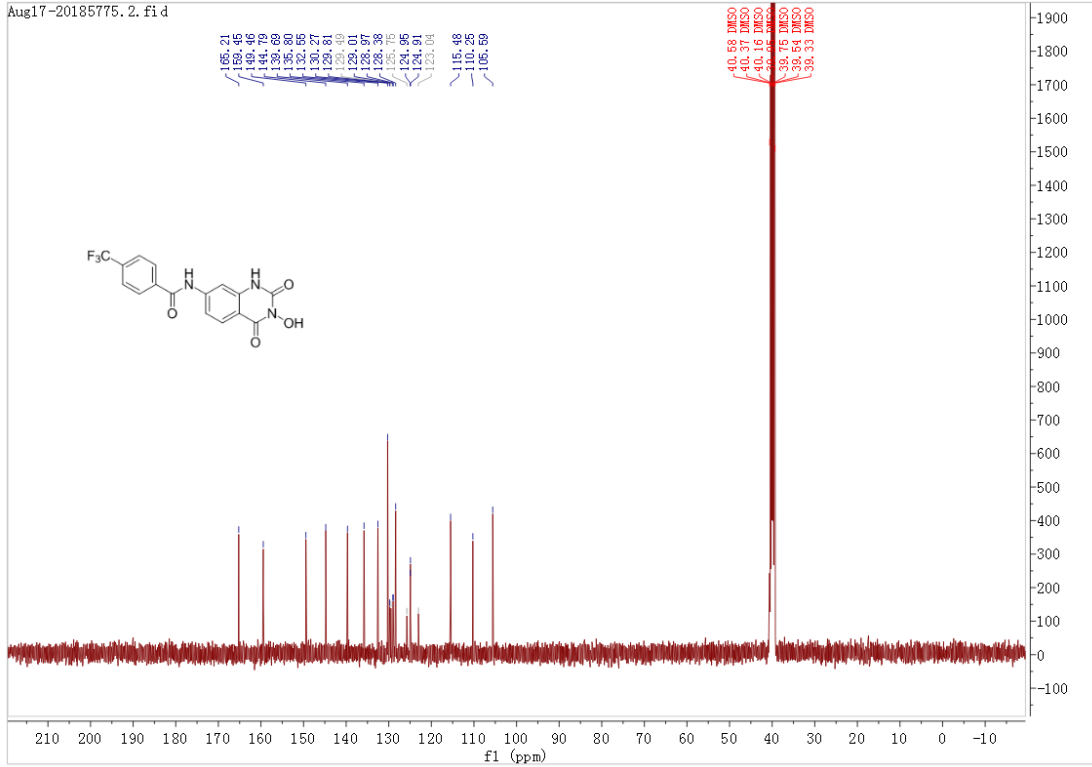
Jun20-20175763.1.f1 d







Aug17-20185775. 2. f1.d



Sep07-20175777-2G

